ACS Chemical Neuroscience

Subscriber access provided by TULANE UNIVERSITY

Article

Novel deoxyvasicinone–donepezil hybrids as potential multitarget drug candidates for Alzheimer's disease

Hong-tao Du, Xinlian Liu, Jusen Xie, and Fang Ma

ACS Chem. Neurosci., **Just Accepted Manuscript** • DOI: 10.1021/acschemneuro.8b00699 • Publication Date (Web): 05 Feb 2019

Downloaded from http://pubs.acs.org on February 7, 2019

Just Accepted

"Just Accepted" manuscripts have been peer-reviewed and accepted for publication. They are posted online prior to technical editing, formatting for publication and author proofing. The American Chemical Society provides "Just Accepted" as a service to the research community to expedite the dissemination of scientific material as soon as possible after acceptance. "Just Accepted" manuscripts appear in full in PDF format accompanied by an HTML abstract. "Just Accepted" manuscripts have been fully peer reviewed, but should not be considered the official version of record. They are citable by the Digital Object Identifier (DOI®). "Just Accepted" is an optional service offered to authors. Therefore, the "Just Accepted" Web site may not include all articles that will be published in the journal. After a manuscript is technically edited and formatted, it will be removed from the "Just Accepted" Web site and published as an ASAP article. Note that technical editing may introduce minor changes to the manuscript text and/or graphics which could affect content, and all legal disclaimers and ethical guidelines that apply to the journal pertain. ACS cannot be held responsible for errors or consequences arising from the use of information contained in these "Just Accepted" manuscripts.

ACS Publications

is published by the American Chemical Society. 1155 Sixteenth Street N.W., Washington, DC 20036

Published by American Chemical Society. Copyright © American Chemical Society. However, no copyright claim is made to original U.S. Government works, or works produced by employees of any Commonwealth realm Crown government in the course of their duties.

Novel deoxyvasicinone–donepezil hybrids as potential multitarget drug candidates for Alzheimer's disease

Hongtao Du [a, d, *], Xinlian Liu [a, b], Jusen Xie [a, b], Fang Ma [c, *]

[a] College of Life Science, Xinyang Normal University, Xinyang, 464000, China

[b] Tea Plant Biology Key Laboratory of Henan Province, Xinyang, 464000, China

[c] School of Geographic Sciences, Xinyang Normal University, Xinyang, 464000, China

[d] College of Plant Protection, Northwest A&F University, Yangling 712100, Shaanxi Province, China

E-mails: duhongtao8410@163.com (H. T. Du); 13782955771@163.com (X. L. Liu); 13782956291@163.com (J. S. Xie); mafang_1984@126.com (F. Ma).

***Corresponding authors:**

Dr. Hongtao Du,

College of Life Science, Xinyang Normal University, Xinyang, 464000, China.

Email: duhongtao8410@163.com

Abstract:

In this study, we designed and synthesized a series of deoxyvasicinone–donepezil hybrids and determined whether they could be used as novel multi-target inhibitors for Alzheimer's disease (AD). *In vitro* studies showed that the most of the hybrids demonstrated moderate to potent inhibition of *h*AChE, BACE1, and A$\beta_{1\text{-}42}$ aggregation. In particular, the hybrids **10*a***, **10*d***, **11*a,*** and **11*j*** exhibited excellent inhibitory activities against *h*AChE (IC_{50} = 56.14 nM, 5.91 nM, 3.29 nM, and 8.65 nM, respectively), BACE1 (IC_{50} = 0.834 μM, 0.167 μM, 0.129 μM, and 0.085 μM, respectively), and A$\beta_{1\text{-}42}$ aggregation (IC_{50} = 13.26 μM, 19.43 μM, 9.26 μM, and 5.41 μM, respectively). In addition, **10*a*** and **11*a*** exhibited very low cytotoxicity and showed remarkable neuroprotective activity against A$\beta_{1\text{-}42}$–induced damage in SH-SY5Y cells.

Keywords: Alzheimer's disease; Acetylcholinesterase; β-secretase; β-amyloid peptide; Deoxyvasicinone

INTRODUCTION

Alzheimer's disease (AD), the most common form of dementia, is a chronic and neurodegenerative illness with a number of symptoms, including loss of memory, deterioration in the use of language, mood swings, and loss of bodily functions leading finally to death.[1-3] Epidemiological data indicate that more than 45 million people suffered from AD in 2015, a number that is projected to triple by 2050.[4] Currently, the most popular drugs for AD include one *N*-methyl-D-aspartate (NMDA) receptor antagonist (memantine) and three cholinesterase (ChE) inhibitors (donepezil, rivastigmine, and galantamine).[5] Unfortunately, these drugs only partially alleviate the symptoms of AD and cannot cure the disease. The exact causes of AD are not yet fully known, but some factors, such as deficits of acetylcholine (ACh), β-amyloid peptide (Aβ) deposits, tauprotein (τ) aggregation, neuroinflammation, and oxidative stress, are suggested to play significant roles in the pathogenesis of AD.[6-9] Due to the complexity of AD and the multitude of factors potentially involved in its progression, a strategy that uses multi-target-directed ligands (MTDLs) has drawn much attention as a mainstream therapeutic approach for treatment of AD.[10-14]

The deposition of Aβ plays a crucial role in the pathogenesis of AD.[15] In particular, A$\beta_{1\text{-}42}$ leads to the formation of senile plaques that causes neuronal death and eventually dementia. The initial and rate-determining step in the production of Aβ is the cleavage of amyloid precursor protein (APP) by β-secretase (BACE1).[16] Therefore, drugs with BACE1 inhibition activity reduce Aβ production and aggregation.[17] Additionally, acetylcholinesterase inhibitors (AChEIs) increase the amount of ACh by blocking acetylcholine hydrolysis in the synaptic cleft.[18] Furthermore, recent studies have shown that AChEIs are able to influence the expression and/or metabolic processing of APP, which may affect Aβ generation.[19] Moreover, some evidence has shown that the peripheral anionic site (PAS) of AChE

contributes to Aβ aggregation.[20] Therefore, we speculate that a single molecule with inhibitory activity against AChE, BACE1, and A$\beta_{1\text{-}42}$ aggregation could be a promising potential agent for AD therapy.

[Fig. 1]

To design novel MTDLs against AD, a pharmacophore-combination strategy was used with deoxyvasicinone and donepezi as the lead compounds. Deoxyvasicinone (Fig. 1), a naturally occurring alkaloid, is composed of a quinazolinone moiety conjugated with pyrrolidine. Its derivatives have been identified as novel cholinesterase inhibitors (Fig. 1).[21-25] We have previously reported a series of deoxyvasicinone derivatives with significant cholinesterase inhibitory activity.[25] These derivatives could bind simultaneously to the catalytic active site (CAS) and the peripheral anionic site (PAS) of *h*AChE. Donepezil is an AChE inhibitor used to treat AD.[5] The benzylpiperidine fragment of donepezil is considered to be a pharmacophore that can bind to the CAS site of AChE.[26-28] In addition, some research has suggested that compounds with an aryl piperazine moiety exhibit significant BACE1 inhibition.[29-31] In the current study, we describe the design, synthesis, and biological evaluation of a series of novel deoxyvasicinone–donepezil hybrids, in which the piperidine fragment of donepezil is replaced by the piperazine moiety (Fig. 2). According to the aforementioned reports, these new deoxyvasicinone–donepezil hybrids may simultaneously possess a dual AChE binding sites for inhibition and inhibitory activity against BACE1 and A$\beta_{1\text{-}42}$ aggregation. Additionally, some target compounds were also evaluated for blood-brain barrier (BBB) permeability and protective capacity for A$\beta_{1\text{-}42}$–induced H-SY5Y cell death. Furthermore, computational studies were performed to predict binding modes in the active pocket.

[Fig. 2]

■ CHEMISTRY

The compounds **8*a*−11*m*** were synthesized as reported in Scheme 1. To obtain deoxyvasicinone (**2**), 2-aminobenzoic acid was reacted with pyrrolidin-2-one analogues using $POCl_3$ as a catalyst in dry toluene. Nitration reaction of deoxyvasicinone (**2**) provided the product, which was reduced to 6-aminodeoxyvasicinone (**3)**. Subsequently, an amidation reaction of the compound **3** with different bromo-acids gave the key intermediates **4**−**7**.[25] Finally, the nucleophilic substitution reaction of compound **4**−**7** with different benzylpiperazine derivatives yielded the target compounds **8*a*−11*m***.

[Scheme 1]

■ RESULTS AND DISCUSSION

In Vitro hAChE and hBuChE Inhibition Assays

Inhibition of *h*AChE and *h*BChE by synthesized derivatives **8*a*−11*m*** was achieved using Ellman's method, wherein tacrine and donepezil were used as reference compounds.[32, 33] First, we screened all of the compounds at a concentration of 1 μM, and IC_{50} values were measured for those with over 50% inhibitory activity against ChEs in the primary screen. The IC_{50} values and their selectivity index are depicted in Table 1.

The tested target compounds showed fascinating inhibitory activity against *h*AChE. Almost all of the compounds display high selectivity for *h*AChE over *h*BChE (except **11*f*)**. Most compounds are potent inhibitors of *h*AChE, with IC_{50} values in the low nanomolar range. Among of them, 13 compounds exhibit significantly higher inhibitory activity than tacrine (IC_{50} = 76.53 nM). Importantly, compounds **9*a***, **9*b***, **10*d***, **11*a***, **11*b***, **11*c***, **11*f***, and **11*i*** have similar or higher inhibitory activity against *h*AChE than donepezil (IC_{50} = 18.54 nM). In particular, compound **11*a*** showed

excellent inhibitory potential and selectivity towards *h*AChE (IC_{50} = 3.29 nM; BuChE/AChE > 303). Furthermore, some structure-activity relationships were surveyed. The length of the alkyl spacer significantly influenced *h*AChE inhibitory activity. Compounds **11*a*−11*d*** (n= 2) exhibited more potent AChE inhibitory than compounds **8*a*−8*d*** (n = 1), compounds **9*a*−9*d*** (n = 3), and compounds **10*a*−10*d*** (n = 4). Thus, lengthening or shortening the alkyl spacer reduced AChE inhibition. In addition, the methyl substituted compounds (except **11*f* *and* 11*g***) showed better inhibitory activity than the corresponding unsubstituted hybrids, when the hybrids had same chain linkers. On the contrary, *h*AChE inhibitory activity decreased in the presence of electron-withdrawing substituents, such as –F, $–CF_3$, –Cl. These results imply that increasing the strength of the electron-donating group could improve *h*AChE inhibitory activity.

BACE1 enzymatic assay

BACE1 inhibitory activity of the synthetic hybrids was tested using a FRET-based assay kit.[29] The inhibitory activity of the test compounds was evaluated at a concentration of 10 μM. The IC_{50} values were then calculated for those with a BACE1 inhibition rate over 50% (Table 1). As shown in Table 1, 17 compounds exhibited good BACE1 inhibitory activity with IC_{50} values ranging from 0.028 μM to 9.03 μM. Notably, 11 hybrids displayed interesting BACE1 inhibitory activity at concentrations below 1 μM. Among them, compounds **9*a*** and **10*c*** are the most potent hybrids against BACE1 (IC_{50} = 0.028 μM and 0.085 μM, respectively), similar to OM99-2 (IC_{50} = 0.016 μM).

Inhibition of $A\beta_{1-42}$ self-aggregation assay

The Thioflavin-T (ThT) fluorescence assay was used to evaluate the inhibitory potency of the derivatives on $A\beta_{1-42}$ self-aggregation.[34] Resveratrol and curcumin were used as controls (Table 1).

Most of compounds exhibited moderate or strong inhibitory activity. The compounds **10*a***, **10*d***, **11*a,*** and **11*j*** exhibited significant inhibition of A$\beta_{1\text{-}42}$ aggregation (IC_{50} =13.26 nM, 19.43 nM, 9.26 nM, and 5.41 nM, respectively), similar to or higher than the inhibitory activity of resveratrol (IC_{50} =10.92 nM) and curcumin (IC_{50} =14.25 nM). Compound **11*j*** displayed the strongest inhibitory activity, 2-fold better than that of resveratrol.

Inhibition of AChE induced Aβ$_{1\text{-}42}$ peptide aggregation assay

Accumulating evidences have indicated that AChE exerts its non-cholinergic function by promoting the aggregation of Aβ peptide, and compounds binding to the PAS of AChE can inhibit AChE accelerated Aβ aggregation. Thus, we evaluated the AChE induced A$\beta_{1\text{-}42}$ aggregation inhibition by compounds **10*a***, **11*a*** and **11*j*** using the ThT assay. As displayed in Fig. 3, A$\beta_{1\text{-}42}$ aggregation was significant decrease after Co-incubation of synthesized compounds and A$\beta_{1\text{-}42}$ with AChE for 24 h. The result clearly demonstrates that these compounds can interfere with the AChE induced A$\beta_{1\text{-}42}$ aggregation.

[Fig. 3]

Kinetic characterization of AChE inhibition

To investigate the mechanistic aspects of inhibition of AChE activity by synthesized compounds, the potent compound **11*a*** was chosen for an enzyme kinetic study. From the Lineweaver-Burk plot (Fig. 4), we observed that both increased slopes (decreased V_{max}) and intercepts (higher K_m) at increasing concentrations of compound **11*a***, indicating a mixed-type inhibition. The result revealed that compound **11*a*** could bind to the CAS as well as the PAS of AChE.

[Fig .4]

In vitro cytotoxicity assay

The compounds **10*a*, 10*d*, 11*a*,** and **11*j*** with potential inhibitory activity against AChE, BACE1, and A$\beta_{1\text{-}42}$ aggregation were selected to evaluate the potential for toxicity in the human neuronal cell line SH-SY5Y. SH-SY5Y cells were exposed to **10*a*, 10*d*, 11*a*,** and **11*j*** at different concentrations (0.1, 1, 10, and 100 μM) for 48 h, and cell viability was determined using the 3-(4,5-dimethylthiazol-2-yl)-2,5-diphenyltetrazolium (MTT) assay.[35] As depicted in Fig. 5A, compounds **10*a***, **11*a***, and **11*j*** show no cytotoxicity at concentrations of 0.1 μM to 1 μM after incubation for 48 h. Compound **11*a*** had no significant effect on cell viability at a concentration of 10 μM. When the concentrations were increased to 100 μM, compounds **10*a*, 11*a***, and **11*j*** displayed significant effects on SH-SY5Y cell viability; however, the cell viability was still above 78%. These results suggest that compounds **10*a*, 11*a***, and **11*j*** exhibit very low toxicity to SH-SY5Y cells in the range of tested concentrations.

To assess hepatotoxicity of synthesized compounds, MTT assay of compounds **10*a***, **11*a*** and **11*j*** on liver hepatocellular cells (HepG2) was performed. As shown in Fig. 5B, compounds **10*a*** and **11*a*** were no cytotoxicity at concentrations of 1– 10 μM after incubation for 48 h. When the concentration of compounds **10*a*** and **11*a*** at 100 μM, the cell viability was still above 88%. Unfortunately, compounds **11*j*** resulted hepatotoxicity at 10 μM concentration, meanwhile a significant reduction of 52 % was observed at 100 μM. These means that compounds **10*a*** and **11*a*** were weakly hepatotoxicity.

[Fig. 5]

The neuroprotective effect of **10*a***, **11*a***, and **11*j*** on A$\beta_{1\text{-}42}$–induced damage in SH-SY5Y cells was assessed using a cell viability assay at three different concentrations: 1 μM, 5 μM, and 10 μM. As shown in Fig. 6, a significant decrease in cell viability (54.5%, $^{\#\#\#}$ $p < 0.001$) was observed when

SH-SY5Y cells were treated with A$\beta_{1\text{-}42}$ for 48 h. However, it is obvious that the tested compounds imparted significant neuroprotection at concentrations between 5 μM and 10 μM. The most potent compound **11*j*** induced marked cellular recovery at the lowest concentration of 1μM (**$p < 0.01$), when compared with the A$\beta_{1\text{-}42}$ treated group. Thus, it seems reasonable to propose that the tested hybrids exhibit neuroprotection against A$\beta_{1\text{-}42}$-induced neurotoxicity through their ability to block A$\beta_{1\text{-}42}$ aggregation.

[Fig. 6]

Physicochemical Properties.

To determine the potential drug-likeness of compounds **10*a***, **11*a***, and **11*j***, their physicochemical properties, such as the calculated octanol/water partition coefficient (*c*Log*P*), topological polar surface area (*t*PSA), the logarithm of brain to blood concentration ratio (LogBB), and the verification of Lipinski's rule of five,[36, 37] were predicted (Table 2). It can be seen that compounds **10*a***, **11*a***, and **11*j*** obey Lipinski's rule of five, fulfill the restrictions of topological polar surface area (*t*PSA), and present good BBB permeability (LogBB). Those results indicate that the selected hybrids (**10*a***, **11*a***, and **11 *j***) are eligible to be orally-available drug candidates for the central nervous system (CNS).

Molecular docking

To further investigate the binding mode of the compounds with their target enzymes, molecular docking simulations of the highest potent hybrid **11*a*** with *h*AChE (PDB code: 4EY7),[38] BACE1 (PDB code: 4D8C),[39] and ***A*$\beta_{1\text{-}42}$** (PDB code: 1IYT)[40] were performed using the Surflex-Dock program in Sybyl-X 2.0 Software (Fig. 7).

As depicted in Fig. 7A. **11*a*** was able to simultaneously bind to both the enzymatic catalytic active site (CAS) and the peripheral anionic site (PAS). This is similar to the way that the amide

group of deoxyvasicinone binds to the PAS through a *cation*−π interaction with Trp286 (3.2 Å), and the carbonyl group creates two hydrogen bonds with residues Phe295 (2.2 Å) and Arg296 (2.1 Å). In mid-gorge sites, a hydrogen bond with the residue Tyr124 (2.0 Å) and a *cation*−π interaction with Phe338 (3.8 Å) were observed, and could enhance the interaction with hAChE. In addition, the benzene ring of piperazine was able to bind to the CAS sites *via* a π−π stacking interaction with Trp86 (3.0 Å). This means that enhancing the electron-donating group of the benzene ring could intensify *h*AChE inhibitory activity, consistent with our previous results.

As shown in Fig. 7B, a *cation*−π interaction was found between residue Try71 and the amino group of piperazine (4.3 Å), which may improve the potency of BACE-1 inhibitory activity. Additionally, the hybrid **11*a*** formed four hydrogen bonds with residues Thr72 (2.99 Å and 3.4 Å), Try18 (3.4 Å) and Gly34 (3.5 Å), which may contribute to improving the interaction between small ligand with BACE1, eventually leading to good inhibitory potency against BACE-1.

Examination of Fig. 7C shows that the benzene ring of piperazine interacts with the residue Phe20 via a π−π stacking interaction at a distance of 3.1 Å. In addition, the carbonyl oxygen and the amino group of piperazine forms hydrogen bonds with Lys16 at distances of 2.1 Å and 2.0 Å respectively, and the amino group of deoxyvasicinone moiety interacts with Gln15 via another hydrogen bond (1.9 Å). These results indicate that the π−π stacking interaction and three hydrogen bond interactions play important roles in the effective inhibition of A$\beta_{1\text{-}42}$ aggregation.

[Fig. 7]

■ CONCLUSIONS

In summary, we designed and synthesized 25 deoxyvasicinone–donepezil hybrids as multi-functional agents for treatment AD. Among them, 13 compounds exhibited similar to or higher

inhibitory activity against *h*AChE than the standard drugs tacrine (IC_{50} = 76.53 nM) and donepezil (IC_{50} = 18.54 nM). Moreover, 17 compounds exhibited good to potential BACE1 inhibitory activities with IC_{50} values from 0.028 μM to 9.03 μM. In addition, the compounds **10*a***, **10*d***, **11*a***, and **11*j*** displayed significant inhibition of A$\beta_{1\text{-}42}$ aggregation (IC_{50} =13.26 nM, 19.43 nM, 9.26 nM, and 5.41 nM, respectively), and possessed good *h*AChE and BACE1 inhibitory activities. Importantly, compounds **10*a***, **11*a***, and **11*j*** showed remarkable neuroprotective activity against A$\beta_{1\text{-}42}$–induced damage in SH-SY5Y cells. In addition, compounds **10*a*** and **11*a*** were low toxicity. Moreover, these compounds should be able to penetrate the blood-brain barrier (BBB). Thus, compounds **10*a*** and **11*a*** should be considered to be effective and promising multi-functional agents against AD.

■ METHODS

General Remarks

All reagents and solvents were obtained from commercial suppliers and used without further purification. Silica GF_{254} for thin-layer chromatography (TLC) were produced by Qingdao Marine Chemical Company (China). Column chromatography was performed on silica gel 200-300 mesh Qingdao Marine Chemical Company (China).

^{1}H NMR and ^{13}C NMR spectra were recorded on a 600 MHz NMR spectrometer （JEOL ECZ600R/S3）equipped with a 14.09 T superconducting magnet and a 5.0 mm 600MHz broadband Z-gradient high resolution ROYAL probe (JEOL RESONANCE Inc., Japan). Chemical shifts are reported in parts per million (ppm, δ) using $CDCl_3$ as solvent and tetramethylsilane (TMS) as a reference. Multiplicities are reported as follows: singlet (s), doublet (d), triplet (t), multiplet (m). High resolution mass spectra (HRMS) were recorded on Agilent 6520 Q-TOF LC/MS and Varian 7.0T FTMS (MALDI).

Preparation of intermediates 2−7

The compound **2** and **3** was synthesized according to a previously described method [25]. Then, a suspension of compound **3** (0.509 g, 2.5 mmol) in dichloromethane (30 mL) was added slowly to a solution of 1-ethyl-3-(3-dimethylaminopropyl)carbodiimide hydrochloride (0.566g, 3 mmol) and bromo-acid (2.7 mmol) in dichloromethane (40 mL). The mixture was refluxed for 24 h and concentrated in vacuum. The reaction solution was washed in order with water, brine, dried over anhyd Na_2SO_4, and concentrated in vacuum to give compound **4**−**7**.

Compound **5**. ^{1}H NMR (600 MHz, Chloroform-*d*) δ 8.68 (s, 1H), 8.29 (dd, *J* = 8.9, 2.5 Hz, 1H), 8.08 (d, *J* = 2.6 Hz, 1H), 7.63 (d, *J* = 8.8 Hz, 1H), 4.26 – 4.18 (m, 2H), 3.76 (t, *J* = 5.6 Hz, 2H), 3.18 (t, *J* = 7.9 Hz, 2H), 2.69 (t, *J* = 5.6 Hz, 2H), 2.35 – 2.26 (m, 2H). ^{13}C NMR (150 MHz, Chloroform-*d*) δ 170.0, 160.8, 158.4, 145.6, 136.6, 127.7, 127.0, 120.7, 115.6, 59.1, 46.5, 37.9, 32.4, 19.6.

Compound **6**. ^{1}H NMR (600 MHz, Chloroform-*d*) δ 8.59 (dd, *J* = 9.0, 2.7 Hz, 1H), 7.97 (d, *J* = 2.6 Hz, 1H), 7.67 (d, *J* = 9.0 Hz, 1H), 4.25 – 4.19 (m, 2H), 3.98 (t, *J* = 7.0 Hz, 2H), 3.19 (t, *J* = 7.9 Hz, 2H), 2.67 (dd, *J* = 8.5, 7.7 Hz, 2H), 2.35 – 2.27 (m, 2H), 2.22 (m, 2H). ^{13}C NMR (150 MHz, Chloroform-*d*) δ 174.5, 160.8, 158.7, 145.7, 137.9, 127.5, 127.2, 120.5, 114.5, 48.9, 46.6, 32.8, 32.4, 19.6, 17.9.

Compound **7**. ^{1}H NMR (600 MHz, Chloroform-*d*) δ 8.45 (s, 1H), 8.39 (dd, *J* = 8.9, 2.5 Hz, 1H), 8.11 (d, *J* = 2.5 Hz, 1H), 7.61 (d, *J* = 8.9 Hz, 1H), 4.19 (t, *J* = 7.3 Hz, 2H), 3.56 (t, *J* = 6.2 Hz, 2H), 3.24 – 3.16 (m, 2H), 2.47 (t, *J* = 7.0 Hz, 2H), 2.36 – 2.28 (m, 2H), 1.94 – 1.84 (m, 4H). ^{13}C NMR (151 MHz, Chloroform-*d*) δ 171.1, 160.8, 158.3, 145.5, 136.9, 127.7, 126.9, 120.5, 115.3, 46.6, 44.6, 36.5, 32.3, 31.9, 22.72, 19.6.

General procedure for the preparation of compounds 8a−11m.

To a stirred solution of compound **4** (161 mg, 0.5 mmol), K_2CO_3 (140 mg, 1 mmol), and 1-benzylpiperazine (176 mg, 1 mmol) in acetonitrile (50 mL) was refluxed. When the compound **4** disappeared (as detected by TLC), the solvents were removed under reduced pressure. Distilled water (25 mL) was then added, and the mixture was extracted with chloroform (20 mL × 3). The organic solvent phase was washed by water (20 mL × 2), brine (20 mL × 2), dried over anhyd Na_2SO_4, and evaporated under vacuum. The compounds **8*a*** were purified by a flash chromatography on silica gel. The compound **8*b*−11*m*** were prepared according to the general procedure.

N-(9-oxo-1,2,3,9-tetrahydropyrrolo[2,1-b]quinazolin-7-yl)-2-(4-benzylpiperazin-1-yl)acetamide (***8a).*** White solid, yield: 63%, m.p. 168−170 °C. ^{1}H NMR (600 MHz, Chloroform-*d*) δ 11.39 (s, 1H), 8.16 (d, *J* = 2.2 Hz, 1H), 8.15 (dd, *J* = 8.7, 2.5 Hz, 1H), 7.61 (d, *J* = 8.7 Hz, 1H), 7.35 – 7.30 (m, 4H), 7.26 (dt, *J* = 7.6, 2.0 Hz, 1H), 3.58 (s, 2H), 3.32– 3.29 (m, 2H), 3.16 (t, *J* = 7.9 Hz, 2H), 2.75 – 2.61 (m, 10H), 2.30 (dt, *J* = 15.2, 8.0 Hz, 2H). ^{13}C NMR (150 MHz, Chloroform-*d*) δ 170.4, 160.4, 157.8, 144.9, 137.5, 136.9, 128.8, 127.9, 127.3, 126.8, 126.4, 120.5, 114.8, 62.5, 60.5, 52.9, 52.1, 46.2, 32.1, 19.5. HRMS (ESI): Calcd. for $C_{24}H_{28}N_5O_2$ $[M+H]^+$ 418.2243, found 418.2239.

N-(9-oxo-1,2,3,9-tetrahydropyrrolo[2,1-b]quinazolin-7-yl)-2-(4-(4-methylbenzyl)piperazin-1-yl)acetamide (**8*b***). White solid, yield: 70 %, m.p. 193−194 °C. ^{1}H NMR (600 MHz, Chloroform-*d*) δ 11.34 (s, 1H), 8.11 (d, *J* = 2.1 Hz, 1H), 8.09 (dd, *J* = 8.6, 2.5 Hz, 1H), 7.54 (d, *J* = 8.7 Hz, 1H), 7.18 (d, *J* = 8.0 Hz, 2H), 7.07 (d, *J* = 7.7 Hz, 2H), 3.49 (s, 2H), 3.29 – 3.25 (m, 2H), 3.10 (t, *J* = 7.9 Hz, 2H), 2.68 – 2.54 (m, 10H), 2.27 (s, 3H), 2.25 (dt, *J* = 15.2, 8.0 Hz, 2H). ^{13}C NMR (150 MHz, Chloroform-*d*) δ169.4, 159.9, 157.6, 144.7, 135.8, 135.4, 133.9, 128.3, 128.1, 126.9, 126.1, 119.9, 114.6, 63.4, 61.7, 52.6, 51.4, 45.6, 31.5, 20.2, 18.7. HRMS (ESI): Calcd. for $C_{25}H_{30}N_5O_2$ $[M+H]^+$ 432.2401, found 432.2395.

N-(9-oxo-1,2,3,9-tetrahydropyrrolo[2,1-b]quinazolin-7-yl)-2-(4-(4-fluorobenzyl)piperazin-1-yl)acetamide (**8*c***). White solid, yield: 48 %, m.p. 186−188 °C. ^{1}H NMR (600 MHz, Chloroform-*d*) δ 11.35 (s, 1H), 8.20 (dd, *J* = 8.8, 2.5 Hz, 1H), 8.11 (d, *J* = 2.5 Hz, 1H), 7.61 (d, *J* = 8.8 Hz, 1H), 7.32 – 7.28 (m, 2H), 7.03 – 6.97 (m, 2H). 3.52 (s, 2H), 3.30– 3.26 (m, 2H), 3.14 (t, *J* = 7.9 Hz, 2H), 2.74 – 2.60 (m, 10H), 2.28 (dt, *J* = 15.2, 8.0 Hz, 2H). ^{13}C NMR (150 MHz, Chloroform-*d*) δ 170.8, 161.8 (d, *J* = 245.0 Hz), 158.3, 144.9, 136.8, 133.4, 130.0, 127.4, 126.5, 120.3, 115.1, 114.9, 62.5, 60.4, 53.0, 51.9, 45.4, 33.1, 19.8. HRMS (ESI): Calcd. for $C_{24}H_{27}FN_5O_2$ $[M+H]^+$ 436.2149, found 436.2136.

N-(9-oxo-1,2,3,9-tetrahydropyrrolo[2,1-b]quinazolin-7-yl)-3-(4-(4-(trifluoromethyl)benzyl)piperazin-1-yl)acetamide (**8*d***). Faint yellow, yield: 65 %, m.p. 153−154 °C. ^{1}H NMR (600 MHz, Chloroform-*d*) δ 11.35 (s, 1H), 8.22 (dd, *J* = 8.8, 2.5 Hz, 1H), 8.13 (d, *J* = 2.5 Hz, 1H), 7.82 (d, *J* = 7.6 Hz, 2H), 7.60 (d, *J* = 8.8 Hz, 1H), 7.20 (d, *J* = 7.6 Hz, 2H), 3.63 (s, 2H), 3.34– 3.30 (m, 2H), 3.16 (t, *J* = 7.9 Hz, 2H), 2.74 – 2.60 (m, 10H), 2.30 (dt, *J* = 15.2, 8.0 Hz, 2H). ^{13}C NMR (150 MHz, Chloroform-*d*) δ 170.3, 160.5, 158.5, 145.2, 139.8, 137.5, 130.3, 129.3, 126.9, 126.7, 124.7, 124.2 (q, *J* = 230 Hz), 120.5, 114.9, 62.6, 60.6, 53.3, 51.9, 45.6, 31.3, 21.0. HRMS (ESI): Calcd. for $C_{26}H_{29}F_3N_5O_2$ $[M+H]^+$ 500.2273, found 500.2261.

N-(9-oxo-1,2,3,9-tetrahydropyrrolo[2,1-b]quinazolin-7-yl)-4-(4-benzylpiperazin-1-yl)butanamide **(9*a*).** White solid, yield: 68 %, m.p. 185−187 °C. ^{1}H NMR (600 MHz, Chloroform-*d*) δ 11.39 (s, 1H), 8.57 (dd, *J* = 9.0, 2.7 Hz, 1H), 7.97 (d, *J* = 2.6 Hz, 1H), 7.66 (d, *J* = 9.0 Hz, 1H), 7.26 – 7.20 (m, 4H), 7.15 – 7.1 (m, 1H), 3.70 (s, 2H), 3.18 (t, *J* = 7.9 Hz, 2H), 2.96 – 2.92 (m, 2H), 2.76 – 2.55 (m, 12H), 2.32 (dt, *J* = 15.2, 8.0 Hz, 2H), 2.04– 1.98 (m, 2H). ^{13}C NMR (150 MHz, Chloroform-*d*) δ 174.5, 160.8, 158.6, 145.7, 137.9, 137.2, 129.1, 128.4, 127.5, 127.1, 126.6, 120.5, 114.5, 62.8, 55.5,

54.2, 52.3, 46.5, 32.7, 32.4, 19.58, 18.9. HRMS (ESI): Calcd. for $C_{26}H_{32}N_5O_2$ $[M+H]^+$ 446.2556, found 446.2560.

N-(9-oxo-1,2,3,9-tetrahydropyrrolo[2,1-b]quinazolin-7-yl)-4-(4-(4-methylbenzyl)piperazin-1-yl)butanamide (**9*b***). White solid, yield: 61 %, m.p. 161−163 °C. ^{1}H NMR (600 MHz, Chloroform-*d*) δ 11.39 (s, 1H), 8.38 (dd, *J* = 9.0, 2.7 Hz, 1H), 7.77 (d, *J* = 2.6 Hz, 1H), 7.58 (d, *J* = 9.0 Hz, 1H), 7.25 (d, *J* = 7.8 Hz, 2H), 7.17 (d, *J* = 7.8 Hz, 2H), 3.72 (s, 2H), 3.19 (t, *J* = 7.9 Hz, 2H), 2.98 – 2.94 (m, 2H), 2.78 – 2.56 (m, 12H), 2.75 (s, 3H), 2.32 (dt, *J* = 15.2, 8.0 Hz, 2H), 2.08 – 2.02 (m, 2H). ^{13}C NMR (150 MHz, Chloroform-*d*) δ 172.8, 160.8, 158.4, 145.4, 137.5, 136.4, 129.2, 128.5, 127.7, 127.1, 126.6, 120.9, 115.3, 62.6, 53.5, 53.3, 52.3, 46.4, 32.4, 32.3, 21.13, 19.5, 18.6. HRMS (ESI): Calcd. for $C_{27}H_{34}N_5O_2$ $[M+H]^+$ 460.2713, found 460.2709.

N-(9-oxo-1,2,3,9-tetrahydropyrrolo[2,1-b]quinazolin-7-yl)-4-(4-(4-fluorobenzyl)piperazin-1-yl)butanamide (**9*c***). White solid, yield: 49 %, m.p. 170−172°C. ^{1}H NMR (600 MHz, Chloroform-*d*) δ 11.41 (s, 1H), 8.18 (dd, *J* = 8.8, 2.5 Hz, 1H), 8.12 (d, *J* = 2.5 Hz, 1H), 7.65 (d, *J* = 8.8 Hz, 1H), 7.34 (dd, *J* = 8.6, 5.5 Hz, 2H), 7.08 (t, *J* = 8.7 Hz, 2H), 3.58 (s, 2H), 3.15 (t, *J* = 7.9 Hz, 2H), 2.98 – 2.94 (m, 2H), 2.78 – 2.64 (m, 12H), 2.39 (dt, *J* = 15.2, 8.0 Hz, 2H), 2.12 – 2.06 (m, 2H). ^{13}C NMR (150 MHz, Chloroform-*d*) δ 170.9, 162.2 (d, *J* = 265.0 Hz), 160.9, 158.3, 145.4, 137.4, 133.8, 130.7, 127.8, 126.9, 121.1, 115.3, 115.2. 63.2, 55.8, 54.6, 52.8, 46.5, 33.7, 31.4, 19.7, 18.2. HRMS (ESI): Calcd. for $C_{26}H_{31}FN_5O_2$ $[M+H]^+$ 464.2462, found 464.2457.

N-(9-oxo-1,2,3,9-tetrahydropyrrolo[2,1-b]quinazolin-7-yl)-4-(4-(4-(trifluoromethyl)benzyl)piperazin-1-yl)butanamide (**9*d***). Faint yellow, yield: 71 %, m.p. 207−209 °C. ^{1}H NMR (600 MHz, Chloroform-*d*) δ 11.38 (s, 1H), 8.22 (dd, *J* = 8.8, 2.5 Hz, 1H), 8.13 (d, *J* = 2.5 Hz, 1H), 7.81 (d, *J* =

7.6 Hz, 2H), 7.63 (d, *J* = 8.8 Hz, 1H), 7.22 (d, *J* = 7.6 Hz, 2H), 3.66 (s, 2H), 3.18 (t, *J* = 7.9 Hz, 2H), 3.02 – 2.98 (m, 2H), 2.78 – 2.58 (m, 12H), 2.35 (dt, *J* = 15.2, 8.0 Hz, 2H), 2.06 – 1.98 (m, 2H). ^{13}C NMR (150 MHz, Chloroform-*d*) δ 170.7, 160.5, 158.3, 145.4, 139.8, 137.4, 130.4, 129.5, 127.1, 126.8, 124.6, 124.1 (q, *J* = 241 Hz), 120.8, 115.2, 62.8, 56.2, 55.3, 52.4, 46.2, 33.1, 30.7, 19.9, 18.8. HRMS (ESI): Calcd. for $C_{27}H_{31}F_3N_5O_2$ $[M+H]^+$ 514.2430, found 514.2422.

N-(9-oxo-1,2,3,9-tetrahydropyrrolo[2,1-b]quinazolin-7-yl)-5-(4-benzylpiperazin-1-yl)pentanami de (**10*a***). White solid, yield: 54 %, m.p. 176−178 °C. ^{1}H NMR (600 MHz, Chloroform-*d*) δ 11.36 (s, 1H), 8.06 (dd, *J* = 8.8, 2.5 Hz, 1H),, 7.69 (d, *J* = 2.5 Hz, 1H), 7.61 (d, *J* = 8.7 Hz, 1H), 7.36 – 7.30 (m, 4H), 7.24 – 7.21 (m, 1H), 3.60 (s, 2H), 3.15 (t, J = 8.0 Hz, 2H), 2.80 – 2.54 (m, 12H), 2.35-2.31 (m, 2H). 2.27 (dt, *J* = 15.2, 8.0 Hz, 2H), 2.02 – 1.94 (m, 4H). ^{13}C NMR (150 MHz, Chloroform-*d*) δ 170.2, 160.5, 159.5, 147.4, 137.8, 141.5, 133.2, 128.5, 127.5, 127.1, 124.0, 120.9, 115.2, 60.8, 55.3, 54.3, 51.3, 44.5, 31.2, 30.8, 19.8, 18.1, 17.2. HRMS (ESI): Calcd. for $C_{27}H_{34}N_5O_2$ $[M+H]^+$ 460.2713, found 460.2719.

N-(9-oxo-1,2,3,9-tetrahydropyrrolo[2,1-b]quinazolin-7-yl)-5-(4-(4-methylbenzyl)piperazin-1-yl)p entanamide (**10*b***). White solid, yield: 66 %, m.p. 169−171 °C. ^{1}H NMR (600 MHz, Chloroform-*d*) δ 11.40 (s, 1H), 8.18 (dd, *J* = 8.8, 2.5 Hz, 1H), 7.88 (d, *J* = 2.5 Hz, 1H), 7.61 (d, *J* = 8.7 Hz, 1H), 7.18 (d, *J* = 8.0 Hz, 2H), 7.09 (d, *J* = 7.7 Hz, 2H), 3.58 (s, 2H), 3.17 (t, J = 8.0 Hz, 2H), 2.80 – 2.54 (m, 12H), 2.38-2.34 (m, 2H). 2.31 (s, 3H), 2.27 (dt, *J* = 15.2, 8.0 Hz, 2H), 2.00 – 1.96 (m, 4H). ^{13}C NMR (150 MHz, Chloroform-*d*) δ 170.5, 160.5, 158.4, 145.6, 137.4, 136.8, 134.6, 129.2, 128.7, 127.5, 126.3, 120.5, 115.0, 61.2, 55.6, 54.3, 51.5, 44.8, 31.4, 30.7, 19.7, 18.3, 17.8, 16.9. HRMS (ESI): Calcd. for $C_{28}H_{36}N_5O_2$ $[M+H]^+$ 474.2869, found 474.2858.

N-(9-oxo-1,2,3,9-tetrahydropyrrolo[2,1-b]quinazolin-7-yl)-5-(4-(4-fluorobenzyl)piperazin-1-yl)pentanamide (**10*c***). White solid, yield: 57 %, m.p. 194−196 °C. ^{1}H NMR (600 MHz, Chloroform-*d*) δ 11.38 (s, 1H), 8.16 (dd, *J* = 8.8, 2.5 Hz, 1H), 7.91 (d, *J* = 2.5 Hz, 1H), 7.62 (d, *J* = 8.8 Hz, 1H), 7.36 (dd, *J* = 8.6, 5.5 Hz, 2H), 7.15 (t, *J* = 8.7 Hz, 2H), 3.62 (s, 2H), 3.17 (t, J = 8.0 Hz, 2H), 2.72 – 2.46 (m, 12H), 2.36-2.32 (m, 2H). 2.28 (dt, *J* = 15.2, 8.0 Hz, 2H), 2.00 – 1.96 (m, 4H). ^{13}C NMR (150 MHz, Chloroform-*d*) δ 170.4, 161.06 (d, *J* = 245.0 Hz), 159.74, 158.39, 146.2, 138.1, 134.2, 131.7, 128.2, 127.36, 120.82, 115.12, 114.81, 61.95, 55.87, 54.90, 50.2, 43.7, 31.8, 29.9, 19.94, 18.6, 18.3, 17.5. HRMS (ESI): Calcd. for $C_{27}H_{33}FN_5O_2$ $[M+H]^+$ 478.2618, found 478.2615.

N-(9-oxo-1,2,3,9-tetrahydropyrrolo[2,1-b]quinazolin-7-yl)-5-(4-(4-(trifluoromethyl)benzyl)piperazin-1-yl)pentanamide (**10*d***). Faint yellow, yield: 65 %, m.p. 211−213 °C. ^{1}H NMR (600 MHz, Chloroform-*d*) δ 11.38 (s, 1H), 8.22 (dd, *J* = 8.8, 2.5 Hz, 1H), 8.13 (d, *J* = 2.5 Hz, 1H), 7.74 (d, *J* = 7.6 Hz, 2H), 7.56 (d, *J* = 8.8 Hz, 1H), 7.16 (d, *J* = 7.6 Hz, 2H), 3.66 (s, 2H), 3.30– 3.28 (m, 2H), 3.18 (t, *J* = 7.9 Hz, 2H), 2.77 – 2.59 (m, 10H), 2.27 (dt, *J* = 15.2, 8.0 Hz, 2H), 2.00 – 1.96 (m, 4H). ^{13}C NMR (150 MHz, Chloroform-*d*) δ 170.5, 160.2, 158.1, 145.1, 139.9, 137.3, 130.5, 129.4, 126.9, 126.8, 124.6, 124.2 (q, *J* = 232 Hz), 120.5, 114.9, 62.1, 55.8, 54.2, 50.7, 43.2, 32.1, 30.7, 19.8, 18.6, 17.7. HRMS (ESI): Calcd. for $C_{28}H_{33}F_3N_5O_2$ $[M+H]^+$ 528.2586, found 528.2579.

N-(9-oxo-1,2,3,9-tetrahydropyrrolo[2,1-b]quinazolin-7-yl)-3-(4-benzylpiperazin-1-yl)propanamide (**11*a***). White solid, yield: 68 %, m.p. 184−185 °C. ^{1}H NMR (600 MHz, Chloroform-*d*) δ 11.41 (s, 1H), 8.23 – 8.14 (m, 2H), 7.62 (d, *J* = 8.7 Hz, 1H), 7.38 – 7.32 (m, 4H), 7.30 – 7.27 (m, 1H), 4.27 – 4.19 (m, 2H), 3.60 (s, 2H), 3.18 (t, *J* = 7.9 Hz, 2H), 2.78 – 2.56 (m, 12H), 2.30 (dt, *J* = 15.2, 8.0 Hz, 2H). ^{13}C NMR (150 MHz, Chloroform-*d*) δ 170.8, 160.7, 158.2, 145.3, 137.9, 137.2, 129.2, 128.3,

127.7, 127.2, 126.7, 120.8, 115.2, 62.9, 53.6, 53.3, 52.4, 46.5, 32.4, 32.4, 19.6. HRMS (ESI): Calcd. for $C_{25}H_{30}N_5O_2$ $[M+H]^+$ 432.2400, found 432.2398.

N-(9-oxo-1,2,3,9-tetrahydropyrrolo[2,1-b]quinazolin-7-yl)-3-(4-(4-methylbenzyl)piperazin-1-yl)propanamide (**11*b***). White solid, yield: 71 %, m.p. 215−216 °C. ^{1}H NMR (600 MHz, Chloroform-*d*) δ 11.39 (s, 1H), 8.20 – 8.08 (m, 2H), 7.59 (d, *J* = 8.7 Hz, 1H), 7.21 (d, *J* = 8.0 Hz, 2H), 7.11 (d, *J* = 7.7 Hz, 2H), 4.25 – 4.14 (m, 2H), 3.52 (s, 2H), 3.15 (t, *J* = 7.9 Hz, 2H), 2.87 – 2.65 (m, 12H), 2.32 (s, 3H), 2.27 (dt, *J* = 15.2, 8.0 Hz, 2H). ^{13}C NMR (150 MHz, Chloroform-*d*) δ 170.7, 160.7, 158.1, 145.2, 137.2, 136.7, 134.8, 129.1, 128.9, 127.6, 126.7, 120.8, 115.1, 62.6, 53.5, 53.3, 52.3, 46.4, 32.4, 32.3, 21.1, 19.5. HRMS (ESI): Calcd. for $C_{26}H_{32}N_5O_2$ $[M+H]^+$ 446.2556, found 446.2552.

N-(9-oxo-1,2,3,9-tetrahydropyrrolo[2,1-b]quinazolin-7-yl)-3-(4-(4-fluorobenzyl)piperazin-1-yl)propanamide (**11*c***). White solid, yield: 69 %, m.p. 148−149 °C. ^{1}H NMR (600 MHz, Chloroform-*d*) δ 11.41 (s, 1H), 8.22 (dd, *J* = 8.8, 2.5 Hz, 1H), 8.13 (d, *J* = 2.5 Hz, 1H), 7.63 (d, *J* = 8.8 Hz, 1H), 7.32 (dd, *J* = 8.6, 5.5 Hz, 2H), 7.02 (t, *J* = 8.7 Hz, 2H), 4.28 – 4.16 (m, 2H), 3.55 (s, 2H), 3.18 (dd, *J* = 8.3, 7.6 Hz, 2H), 2.81 – 2.62 (m, 12H), 2.30 (dt, *J* = 15.2, 8.0 Hz, 2H). ^{13}C NMR (150 MHz, Chloroform-*d*) δ 170.7, 162.0 (d, *J* = 245.0 Hz), 160.7, 158.1, 145.3, 137.2, 133.7, 130.5, 127.6, 126.7, 120.8, 115.1, 115.1, 62.0, 53.5, 53.2, 52.3, 46.4, 32.4, 32.3, 19.6. HRMS (ESI): Calcd. for $C_{25}H_{29}FN_5O_2$ $[M+H]^+$ 450.2305, found 450.2303.

N-(9-oxo-1,2,3,9-tetrahydropyrrolo[2,1-b]quinazolin-7-yl)-3-(4-(4-(trifluoromethyl)benzyl)piperazin-1-yl)propanamide (**11*d***). Faint yellow, yield: 75 %, m.p. 173−174 °C. ^{1}H NMR (600 MHz, Chloroform-*d*) δ 11.38 (s, 1H), 8.20 (dd, *J* = 8.8, 2.5 Hz, 1H), 8.11 (d, *J* = 2.5 Hz, 1H), 7.72 (d, *J* = 7.6 Hz, 2H), 7.58 (d, *J* = 8.8 Hz, 1H), 7.18 (d, *J* = 7.6 Hz, 2H), 4.26 – 4.12 (m, 2H), 3.69 (s, 2H),

3.19 (t, *J* = 7.9 Hz, 2H), 2.84– 2.62 (m, 12H), 2.28 (dt, *J* = 15.2, 7.9 Hz, 2H). ^{13}C NMR (150 MHz, Chloroform-*d*) δ 170.6, 160.7, 158.2, 145.3, 139.8, 137.4, 130.4, 129.5, 126.9, 126.8, 124.8, 124.3 (q, *J* = 227 Hz), 120.8, 115.1, 62.2, 53.5, 53.3, 52.3, 46.4, 32.4, 32.3, 19.5. HRMS (ESI): Calcd. for $C_{26}H_{29}F_3N_5O_2$ $[M+H]^+$ 500.2273, found 500.2268.

N-(9-oxo-1,2,3,9-tetrahydropyrrolo[2,1-b]quinazolin-7-yl)-3-(4-(4-chlorobenzyl)piperazin-1-yl)propanamide (**11*e***). Yellow, yield: 52 %, m.p. 195−197 °C. ^{1}H NMR (600 MHz, Chloroform-*d*) δ 11.40 (s, 1H), 8.20 (dd, *J* = 8.8, 2.5 Hz, 1H), 8.12 (d, *J* = 2.5 Hz, 1H), 7.59 (d, *J* = 8.7 Hz, 1H), 7.43 (d, *J* = 8.0 Hz, 2H), 7.29 (d, *J* = 7.7 Hz, 2H), 4.26 – 4.14 (m, 2H), 3.60 (s, 2H), 3.18 (t, *J* = 7.9 Hz, 2H), 2.86 – 2.40 (m, 12H), 2.27 (dt, *J* = 15.2, 8.0 Hz, 2H). ^{13}C NMR (150 MHz, Chloroform-*d*) δ 170.5, 160.3, 158.3, 145.4, 137.5, 136.8, 132.4, 130.2, 128.6, 127.1, 126.5, 120.1, 115.1, 62.2, 53.3, 53.1, 52.5, 46.8, 32.2, 31.4, 19.8. HRMS (ESI): Calcd. for $C_{25}H_{29}ClN_5O_2$ $[M+H]^+$ 466.2010, found 466.2009.

N-(9-oxo-1,2,3,9-tetrahydropyrrolo[2,1-b]quinazolin-7-yl)-3-(4-(3-methylbenzyl)piperazin-1-yl)propanamide (**11*f***). White solid, yield: 77 %, m.p. 206−208 °C. ^{1}H NMR (600 MHz, Chloroform-*d*) δ 11.38 (s, 1H), 8.20 (d, *J* = 2.5 Hz, 1H), 8.14 (dd, *J* = 8.8, 2.5 Hz, 1H), 7.62 (d, *J* = 8.8 Hz, 1H), 7.22 (t, *J* = 7.5 Hz, 1H), 7.19 – 7.13 (m, 2H), 7.09 (d, *J* = 7.4 Hz, 1H), 4.29 – 4.16 (m, 2H), 3.56 (s, 2H), 3.18 (t, *J* = 7.9 Hz, 2H), 2.80 – 2.60 (m, 12H), 2.35 (s, 3H), 2.30 (dt, *J* = 15.2, 8.0 Hz, 2H). ^{13}C NMR (150 MHz, Chloroform-*d*) δ 170.7, 160.7, 158.2, 145.2, 137.9, 137.6, 137.2, 129.9, 128.2, 128.0, 127.6, 126.7, 126.3, 120.8, 115.2, 62.9, 53.5, 53.2, 52.3, 46.5, 32.4, 32.3, 21.4, 19.6. HRMS (ESI): Calcd. for $C_{26}H_{32}N_5O_2$ $[M+H]^+$ 446.2556, found 446.2558.

N-(9-oxo-1,2,3,9-tetrahydropyrrolo[2,1-b]quinazolin-7-yl)-3-(4-(3-fluorobenzyl)piperazin-1-yl)p

ropanamide (**11*g***). White solid, yield: 48 %, m.p. 216−217 °C. ^{1}H NMR (600 MHz, Chloroform-*d*) δ 11.39 (s, 1H), 8.20 (dd, *J* = 8.8, 2.5 Hz, 1H), 8.15 (d, *J* = 2.5 Hz, 1H), 7.63 (d, *J* = 8.8 Hz, 1H), 7.31 – 7.26 (m, 1H), 7.16 – 7.09 (m, 2H), 6.95-6.92 (m, 1H), 4.29 – 4.18 (m, 2H), 3.58 (s, 2H), 3.18 (t, *J* = 7.9 Hz, 2H), 2.78 – 2.56 (m, 12H), 2.30 (dt, *J* = 15.2, 8.0 Hz, 2H). ^{13}C NMR (150 MHz, Chloroform-*d*) δ 170.7, 162.9 (d, *J* = 245.6 Hz), 160.7, 158.2, 145.2, 140.8, 137.2, 129.7, 127.6, 126.7, 124.5, 120.8, 115.6, 115.1, 114.0, 62.2, 53.5, 53.3, 52.3, 46.4, 32.4, 32.3, 19.6. HRMS (ESI): Calcd. for $C_{25}H_{29}FN_5O_2$ $[M+H]^+$ 450.2305, found 450.2313.

N-(9-oxo-1,2,3,9-tetrahydropyrrolo[2,1-b]quinazolin-7-yl)-3-(4-(3-(trifluoromethyl)benzyl)piper azin-1-yl)propanamide (**11*h***). Faint yellow, yield: 64 %, m.p. 193−195 °C. ^{1}H NMR (600 MHz, Chloroform-*d*) δ 11.38 (s, 1H), 8.22 (dd, *J* = 8.8, 2.5 Hz, 1H), 8.14 (d, *J* = 2.5 Hz, 1H), 7.64 (s, 1H), 7.63 (d, *J* = 8.8 Hz, 1H), 7.54 (dd, *J* = 14.0, 7.7 Hz, 2H), 7.45 (t, *J* = 7.7 Hz, 1H), 4.28 – 4.18 (m, 2H), 3.64 (s, 2H), 3.18 (t, *J* = 7.9 Hz, 2H), 2.86 – 2.63 (m, 12H), 2.30 (dt, *J* = 15.2, 7.9 Hz, 2H). ^{13}C NMR (150 MHz, Chloroform-*d*) δ 170.7, 160.7, 158.2, 145.3, 139.2, 137.2, 132.3, 130.6, 128.7, 127.6, 126.7, 125.5, 124.2(q, *J* = 231.9 Hz), 124.0, 120.8, 115.1, 62.2, 53.5, 53.3, 52.3, 46.4, 32.4, 32.3, 19.5. HRMS (ESI): Calcd. for $C_{26}H_{29}F_3N_5O_2$ $[M+H]^+$ 500.2273, found 500.2271.

N-(9-oxo-1,2,3,9-tetrahydropyrrolo[2,1-b]quinazolin-7-yl)-3-(4-(3-chlorobenzyl)piperazin-1-yl)p ropanamide (**11*i***). Yellow, yield: 55 %, m.p. 166−168 °C. ^{1}H NMR (600 MHz, Chloroform-*d*) δ 11.39 (s, 1H), 8.18 (dd, *J* = 8.8, 2.5 Hz, 1H), 8.12 (d, *J* = 2.5 Hz, 1H), 7.68 (s, 1H), 7.61 (d, *J* = 8.8 Hz, 1H), 7.30 – 7.26 (m, 2H), 6.96 (tdd, *J* = 8.4, 2.6, 1.0 Hz, 1H), 4.26 – 4.14 (m, 2H), 3.62 (s, 2H), 3.18 (t, *J* = 7.9 Hz, 2H), 2.80 – 2.59 (m, 12H), 2.30 (dt, *J* = 15.2, 8.0 Hz, 2H). ^{13}C NMR (150 MHz, Chloroform-*d*) δ 170.7, 162.9 (d, *J* = 245.6 Hz), 160.7, 158.2, 145.2, 140.8, 137.2, 129.7, 127.6, 126.7, 124.5, 120.8, 115.6, 115.1, 114.0, 62.2, 53.5, 53.3, 52.3, 46.4, 32.4, 32.3, 19.6. HRMS (ESI):

Calcd. for $C_{25}H_{29}ClN_5O_2$ $[M+H]^+$ 466.2010, found 466.2012.

N-(9-oxo-1,2,3,9-tetrahydropyrrolo[2,1-b]quinazolin-7-yl)-3-(4-(2-methylbenzyl)piperazin-1-yl)propanamide (**11*j***). White solid, yield: 62 %, m.p. 207−209 °C. ^{1}H NMR (600 MHz, Chloroform-*d*) δ 11.42 (s, 1H), 8.25 – 8.16 (m, 2H), 7.64 (d, *J* = 8.7 Hz, 1H), 7.28 (d, *J* = 7.2 Hz, 1H), 7.21 – 7.13 (m, 3H), 4.30 – 4.12 (m, 2H), 3.55 (s, 2H), 3.18 (t, *J* = 7.9 Hz, 2H), 2.78 – 2.56 (m, 11H), 2.39 (s, 3H), 2.30 (dt, *J* = 15.2, 7.9 Hz, 2H). ^{13}C NMR (150 MHz, Chloroform-*d*) δ 170.8, 160.7, 158.2, 145.2, 137.6, 137.2, 136.1, 130.3, 129.8, 127.6, 127.2, 126.8, 125.5, 120.8, 115.2, 60.7, 53.6, 53.2, 52.5, 46.5, 32.4, 32.3, 19.6, 19.2. HRMS (ESI): Calcd. for $C_{26}H_{32}N_5O_2$ $[M+H]^+$ 446.2556, found 446.2551.

N-(9-oxo-1,2,3,9-tetrahydropyrrolo[2,1-b]quinazolin-7-yl)-3-(4-(2-fluorobenzyl)piperazin-1-yl)-propanamide (**11*k***). White solid, yield: 49 %, m.p. 187−188 °C. ^{1}H NMR (600 MHz, Chloroform-*d*) δ 11.33 (s, 1H), 8.25 (d, *J* = 2.5 Hz, 1H), 8.03 (dd, *J* = 8.8, 2.5 Hz, 1H), 7.60 (d, *J* = 8.8 Hz, 1H), 7.40 (td, *J* = 7.5, 1.8 Hz, 1H), 7.29 – 7.25 (m, 1H), 7.13 (td, *J* = 7.5, 1.2 Hz, 1H), 7.06 (ddd, *J* = 9.6, 8.2, 1.2 Hz, 1H), 4.30 – 4.14 (m, 2H), 3.66 (d, *J* = 1.3 Hz, 2H), 3.18 (t, *J* = 7.9 Hz, 2H), 2.78 – 2.56 (m, 12H), 2.30 (dt, *J* = 15.2, 7.9 Hz, 2H). ^{13}C NMR (150 MHz, Chloroform-*d*) δ 170.7, 161.4 (d, *J* = 246.5 Hz), 160.6, 158.2, 145.2, 137.1, 131.5, 129.0, 127.5, 126.6, 124.4, 123.9, 120.8, 115.3, 115.3, 55.2, 53.5, 53.1, 52.2, 46.5, 32.4, 32.3, 19.5. HRMS (ESI): Calcd. for $C_{25}H_{29}FN_5O_2$ $[M+H]^+$ 450.2305, found 450.2302.

N-(9-oxo-1,2,3,9-tetrahydropyrrolo[2,1-b]quinazolin-7-yl)-3-(4-(2-(trifluoromethyl)benzyl)piperazin-1-yl)propanamide (**11*l***). Faint yellow, yield: 70 %, m.p. 177−179 °C. ^{1}H NMR (600 MHz, Chloroform-*d*) δ 11.24 (s, 1H), 8.21 (d, *J* = 2.5 Hz, 1H), 8.08 (dd, *J* = 8.8, 2.5 Hz, 1H), 7.74 (d, *J* =

7.7 Hz, 1H), 7.61 (t, *J* = 7.9 Hz, 2H), 7.50 (t, *J* = 7.5 Hz, 1H), 7.33 (t, *J* = 7.6 Hz, 1H), 4.26 – 4.13 (m, 2H), 3.73 (s, 2H), 3.15 (t, *J* = 7.9 Hz, 2H), 2.85 – 2.61 (m, 12H), 2.30 (dt, *J* = 15.2, 7.9 Hz, 2H). ^{13}C NMR (150 MHz, Chloroform-*d*) δ 170.7, 160.7, 158.2, 145.3, 137.4, 137.0, 131.7, 130.3, 128.7, 127.6, 126.9, 126.8, 125.9, 124.3 (q, *J* = 227.5 Hz), 120.8, 115.4, 58.1, 53.7, 53.3, 52.5, 46.5, 32.4, 32.3, 19.5. HRMS (ESI): Calcd. for $C_{26}H_{29}F_3N_5O_2$ $[M+H]^+$ 500.2273, found 500.2265.

N-(9-oxo-1,2,3,9-tetrahydropyrrolo[2,1-b]quinazolin-7-yl)-3-(4-(2-chlorobenzyl)piperazin-1-yl)propanamide (**11*m***). Faint yellow, yield: 68 %, m.p. 213−215 °C. ^{1}H NMR (600 MHz, Chloroform-*d*) δ 11.33 (s, 1H), 8.20 (d, *J* = 2.5 Hz, 1H), 8.05 (dd, *J* = 8.8, 2.5 Hz, 1H), 7.60 (d, *J* = 8.8 Hz, 1H), 7.42(d, *J* = 7.5, 1H), 7.26 – 7.23 (m, 1H), 7. 22-7.18 (m, 2H), 4.28 – 4.14 (m, 2H), 3.64 (d, *J* = 1.3 Hz, 2H), 3.18 (t, *J* = 7.9 Hz, 2H), 2.80 – 2.62 (m, 12H), 2.27 (dt, *J* = 15.2, 7.9 Hz, 2H). ^{13}C NMR (150 MHz, Chloroform-*d*) δ 170.7, 160.6, 158.4, 145.2, 137.6, 136.5, 134.4, 130.5, 128.7, 128.3, 127.4, 126.3, 125.6, 120.7, 115.1, 61.3, 54.8, 53.6, 52.7, 46.8, 32.9, 32.4, 19.9. HRMS (ESI): Calcd. for $C_{25}H_{29}ClN_5O_2$ $[M+H]^+$ 466.2010, found 466.2015.

In vitro hAChE and hBuChE inhibition assay

Inhibitory activity was measured using Ellman's assay.[32] *h*AChE (form human erythrocytes), *h*BuChE (from human serum), 5,5′-dithiobis(2-nitrobenzoic acid) (DTNB), acetylthiocholine iodide (ATCI), and butyrylthiocholine iodide (BTCI) were obtained from Sigma-Aldrich. The assay was performed as described in the following procedure: At least 5 different concentrations (1×10^{-5}–10^{-9} M) of each test compound were measured, each concentration in triplicate. Then, 50 μL of *h*AChE (0.02 unit/mL) or *h*BChE (0.02 unit/mL) and 10 μL of the compound was incubated at 37°C for 6 min; next, 30 μL of 0.01 M substrate (ATCI or BTCI solution) was added, and the solution was further incubated at 37°C for 12 min. Finally, 150 μL of 0.01 M DTNB was added, and the activity

was measured at a wavelength of 415 nm using an Evolution 300 PC UV-Vis Spectrophotometer. The IC_{50} value was calculated using Origin 8.0 software.

BACE1 enzymatic assay

Human BACE1 activity was assayed using a BACE1 (β-secretase) FRET (Fluorescense Resonance Energy Transfer) assay kit.[33] OM99-2 was used in the assay as a positive control. The test compounds were dissolved in DMSO and further diluted with the assay buffer (50 mM sodium acetate; pH 4.5). 10 μL of BACE1 enzyme (1 Units/mL) and 10 μL of each tested compound were placed in 96-well plates. Then, 10 μL of BACE1 substrate (Rh-EVNLDAEFK-Quencher) was added to start the reaction (the final concentration of DMSO in each sample and control wells was equal or less than 5%). The mixture was incubated at room temperature for 1 h in the dark, and 10 μL of 2.5 M sodium acetate was then applied to stop the reaction. The fluorescence was monitored at 545 nm (excitation wave length, Exc) and 585 nm (emission wavelength, Em).

A$\beta_{1\text{-}42}$ self-aggregation inhibition assay

Inhibition of A$\beta_{1\text{-}42}$ self-aggregation was measured using the thioflavin T fluorescence method.[34] 1,1,1,3,3,3-hexafluoro-2-propanol (HFIP) pretreated A$\beta_{1\text{-}42}$ samples (Sigma-Aldrich) were dissolved with PBS (pH 7.4) to give a 40 mM solution. Meanwhile, the ThT solution was prepared in PBS (pH 7.4) at a concentration of 10 μM. Then, 10 μL of 40 μM A$\beta_{1\text{-}42}$ solution was added to each well containing 10 μL of different concentrations of test compounds. After incubation at 30 °C for 24 h, the samples were diluted to a final volume of 200 μL with ThT solution. Then, a 300 s time scan of fluorescence intensity was performed (λ_{exc} = 446 nm; λ_{em} = 490 nm), and values at plateau were averaged after subtracting the background fluorescence of the thioflavin T solution.

Kinetic characterization of AChE inhibition

To measure the mechanism of AChE inhibition by synthesized compounds, different concentrations of compound **11*a***.(1 – 10 nM) were reacted with different substrate (AChE) oncentrations (0.1 – 0.5 mM). Then, the V_m and K_m values of the inhibition were measured by plotting the Lineweaver-Burk plot.

Inhibition of AChE induced $A\beta_{1-42}$ peptide aggregation assay

Inhibition of AChE induced $A\beta_{1-42}$ peptide aggregation were conducted by co-incubation of synthesized compounds (1 μM and 5 μM) and $A\beta_{1-42}$ peptide with AChE (10 μM). For control experiment, the test compound is absent. We have monitored the aggregation of $A\beta_{1-42}$ peptide by ThT at 37 °C for 24 h . The excitation wavelength was 446 nm and emission was ranging between 490 nm

In vitro cytotoxicity assay

The human neuroblastoma SH-SY5Y and HepG2 cell lines were obtained from the Procell Life Science & Technology Co., Ltd. Cells were grown in Dulbecco's modified Eagle's medium (DMEM) containing 10% (*v*/*v*) fetal bovine serum (FBS, Hyclone), 50 U/mL penicillin, and 50 mg/mL streptomycin, under a humidified atmosphere of 5% CO_2 at 37 °C. The toxic effects of the compounds were assessed using an MTT (3-(4,5-dimethylthiazol-2-yl)-2,5- diphenyltetrazolium bromide) assay as described previousl.[35] Briefly, SH-SY5Y or HepG2 cells were seeded in 96-well plates at 1×10^4 per well and cultured at 37 °C for 24 h. Then, cells were exposed to the tested compounds at various concentrations (0.1–100 μM) for 48 h. The final concentration of DMSO in culture media did not exceed 0.05% (*v*/*v*) and no alterations of the cells were observed. The MTT reagent was added to each well and incubated for an additional 4 h followed by solubilization of formazan crystals in DMSO. Absorbance was measured at 570 nm using a microculture plate reader.

Protection of SH-SY5Y cells against $A\beta_{1-42}$–induced damage

SH-SY5Y cells were seeded in 96-well plates at 1×10^4 per well and cultured at 37°C for 24 h. $A\beta_{1-42}$ **(**20 μM**)** with or without test compounds **10a**, **11a**, and **11j (**1 μM, 5 μM, and 10 μM**)** were diluted with medium and added into individual wells. Then, plates were again incubated for an additional 48 h at 37 °C. Cell viability was determined using MTT assay protocol, and expressed as a percentage of the control cells.

Molecular docking

Docking was performed by using the Surflex-Dock program in Sybyl-X 2.0 Software. The 3D structures of ligands were drawn in the Sybyl package. Atom types were checked, hydrogen atoms were added, and then Gasteiger-Marsili charges were assigned with Sybyl-X 2.0 Software. The protein structures of *h*AChE (PDB code: 4EY7), BACE1 (PDB code: 4D8C), and $A\beta_{1-42}$ (PDB code: 1IYT) were derived from the RCSB Protein Data Bank (https://www.rcsb.org/). To conduct molecular docking studies, the ligand of the crystal structure was extracted, hydrogen atoms were added, and side-chain amides were checked. Then, the protomol was generated. PyMOL was used to visualize the results of docking.[41]

■ AUTHOR INFORMATION

Corresponding Authors

*Tel: +86-0376- 6391565. E-mail: wangjunru@nwsuaf.edu.cn

Author Contributions

Hongtao Du and Fang Ma take charge of the research; Fang Ma and Xinlian Liu synthesized compounds; Hongtao Du and Jusen Xie carried out biological activity tests. Hongtao Du and Fang Ma written the manuscript. All authors have given approval to the final version of the manuscript.

Acknowledgments

This work was supported by grants from the Program for Natural Science Foundation of China (Grant No. 21602178), Nanhu Scholars Program for Young Scholars of XYNU, and the study and utilization of active components of special plants (Grant No. 2018083). We thank Dr. qiuju Zhou (Analysis and Testing Center, Xinyang Normal University) for her help in the compounds structure analyses. We also thank LetPub (www.letpub.com) for its linguistic assistance during the preparation of this manuscript.

Conflicts of interest

The authors declare no conflict of interest about this article.

REFERENCES

1. Goedert, M., and Spillantini, M. G. (2006) A century of Alzheimer's disease, *Science 314*, 777-781.

2. Mendiola-Precoma, J., Berumen, L. C., Padilla, K., and Garcia-Alcocer, G. (2016) Therapies for Prevention and Treatment of Alzheimer's Disease, *BioMed Res. Int.,2016,* 2589276.

3. Prati, F., Bottegoni, G., Bolognesi, M. L., and Cavalli, A. (2018) BACE-1 Inhibitors: From Recent Single-Target Molecules to Multitarget Compounds for Alzheimer's Disease, *J. Med. Chem. 61*, 619-637.

4. The Global Voice on Dementia, Alzheimer's Disease International, World Alzheimer Report. https://www.alz.co.uk/research/WorldAlzheimerReport2016.pdf (accessed April 24, 2016).

5. Tan, C.-C., Yu, J.-T., Wang, H.-F., Tan, M.-S., Meng, X.-F., Wang, C., Jiang, T., Zhu, X.-C., and Tan, L. (2014) Efficacy and Safety of Donepezil, Galantamine, Rivastigmine, and Memantine for the Treatment of Alzheimer's Disease: A Systematic Review and Meta-Analysis, *J. Alzheimers Dis. 41*, 615-631.

6. Isacson, O., Seo, H., Lin, L., Albeck, D., and Granholm, A. C. (2002) Alzheimer's disease and Down's syndrome: roles of APP, trophic factors and ACh, *Trends Neurosci. 25*, 79-84.

7. Ittner, L. M., and Goetz, J. (2011) Amyloid-beta and tau - a toxic pas de deux in Alzheimer's disease, *Nat. Rev. Neurosci. 12*, 67-72.

8. Roberson, E. D., Scearce-Levie, K., Palop, J. J., Yan, F., Cheng, I. H., Wu, T., Gerstein, H., Yu, G.-Q., and Mucke, L. (2007) Reducing endogenous tau ameliorates amyloid beta-induced deficits in an Alzheimer's disease mouse model, *Science 316*, 750-754.

9. Cheignon, C., Tomas, M., Bonnefont-Rousselot, D., Faller, P., Hureau, C., and Collin, F. (2018) Oxidative stress and the amyloid beta peptide in Alzheimer's disease, *Redox Biol. 14*, 450-464.

10. Spangenberg, E. E., and Green, K. N. (2017) Inflammation in Alzheimer's disease: Lessons learned from microglia-depletion models, *Brain Behav. Immun. 61*, 1-11.

11. Deora, G. S., Kantham, S., Chan, S., Dighe, S. N., Veliyath, S. K., McColl, G., Parat, M.-O., McGeary, R. P., and Ross, B. P. (2017) Multifunctional Analogs of Kynurenic Acid for the Treatment of Alzheimer's Disease: Synthesis, Pharmacology, and Molecular Modeling Studies, *Acs Chemical Neuroscience 8*, 2667-2675.

12. Hiremathad, A., Keri, R. S., Esteves, A. R., Cardoso, S. M., Chaves, S., and Santos, M. A. (2018) Novel Tacrine-Hydroxyphenylbenzimidazole hybrids as potential multitarget drug candidates for Alzheimer's disease, *Eur. J. Med. Chem. 148*, 255-267.

13. Kumar, B., Dwivedi, A. R., Sarkar, B., Gupta, S. K., Krishnamurthy, S., Mantha, A. K., Parkash, J., and Kumar, V. (2018) 4,6-Diphenylpyrimidine Derivatives as Dual Inhibitors of Monoamine Oxidase and Acetylcholinesterase for the Treatment of Alzheimer's Disease, *Acs Chem. Neurosci.* DOI: 10.1021/acschemneuro.8b00220.

14. Li, X., Wang, H., Xu, Y., Liu, W., Gong, Q., Wang, W., Qiu, X., Zhu, J., Mao, F., Zhang, H., and Li, J. (2017) Novel Vilazodone Tacrine Hybrids as Potential Multitarget-Directed Ligands for the Treatment of Alzheimer's Disease Accompanied with Depression: Design, Synthesis, and Biological Evaluation, *Acs Chem. Neurosci. 8*, 2708-2721..

15. Sevigny, J., Chiao, P., Bussiere, T., Weinreb, P. H., Williams, L., Maier, M., Dunstan, R., Salloway, S., Chen, T.,

Ling, Y., O'Gorman, J., Qian, F., Arastu, M., Li, M., Chollate, S., Brennan, M. S., Quintero-Monzon, O., Scannevin, R. H., Arnold, H. M., Engber, T., Rhodes, K., Ferrero, J., Hang, Y., Mikulskis, A., Grimm, J., Hock, C., Nitsch, R. M., and Sandrock, A. (2016) The antibody aducanumab reduces A beta plaques in Alzheimer's disease, *Nature 537*, 50-56.

16. Scheuner, D., Eckman, C., Jensen, M., Song, X., Citron, M., Suzuki, N., Bird, T. D., Hardy, J., Hutton, M., Kukull, W., Larson, E., LevyLahad, E., Viitanen, M., Peskind, E., Poorkaj, P., Schellenberg, G., Tanzi, R., Wasco, W., Lannfelt, L., Selkoe, D., and Younkin, S. (1996) Secreted amyloid beta-protein similar to that in the senile plaques of Alzheimer's disease is increased in vivo by the presenilin 1 and 2 and APP mutations linked to familial Alzheimer's disease, *Nat. Med 2*, 864-870.
17. Sun, J., and Roy, S. (2018) The physical approximation of APP and BACE-1: A key event in alzheimer's disease pathogenesis, *Dev. Neurobio. 78*, 340-347.
18. Jalili-Baleh, L., Nadri, H., Moradi, A., Bukhari, S. N. A., Shakibaie, M., Jafari, M., Golshani, M., Moghadam, F. H., Firoozpour, L., Asadipour, A., Emami, S., Khoobi, M., and Foroumadi, A. (2017) New racemic annulated pyrazolo 1,2-b phthalazines as tacrine-like AChE inhibitors with potential use in Alzheimer's disease, *Eur. J. Med. Chem. 139*, 280-289.
19. Zhao, X. J., Gong, D. M., Jiang, Y. R., Guo, D., Zhu, Y., and Deng, Y. C. (2017) Multipotent AChE and BACE-1 inhibitors for the treatment of Alzheimer's disease: Design, synthesis and bio-analysis of 7-amino-1,4-dihydro-2H-isoquilin-3-one derivates, *Eur. J. Med. Chem. 138*, 738-747.
20. Yang, X., Qiang, X., Li, Y., Luo, L., Xu, R., Zheng, Y., Cao, Z., Tan, Z., and Deng, Y. (2017) Pyridoxine-resveratrol hybrids Mannich base derivatives as novel dual inhibitors of AChE and MAO-B with antioxidant and metal-chelating properties for the treatment of Alzheimer's disease, *Bioorg. Chem. 71*, 305-314.
21. Darras, F. H., Pockes, S., Huang, G., Wehle, S., Strasser, A., Wittmann, H. J., Nimczick, M., Sotriffer, C., and

Decker, M. (2014) Synthesis, Biological Evaluation, and ComputationalStudies of Tri- and Tetracyclic Nitrogen-Bridgehead Compounds as PotentDual-Acting AChE Inhibitors and hH3 ReceptorAntagonists, *Acs Chem. Neurosci. 5*, 225-242.

22. Darras, F. H., Kling, B., Heilmann, J., and Decker, M. (2012) Neuroprotective Tri- and Tetracyclic BChE Inhibitors Releasing Reversible Inhibitors upon Carbamate Transfer, *Acs Med. Chem. Lett. 3*, 914-919.

23. Darras, F. H., Wehle, S., Huang, G., Sotriffer, C. A., and Decker, M. (2014) Amine substitution of quinazolinones leads to selective nanomolar AChE inhibitors with 'inverted' binding mode, *Bioorgan. Med. Chem. 22*, 4867-4881.

24. Yan, J.-W., Li, Y.-P., Ye, W.-J., Chen, S.-B., Hou, J.-Q., Tan, J.-H., Ou, T.-M., Li, D., Gu, L.-Q., and Huang, Z.-S. (2012) Design, synthesis and evaluation of isaindigotone derivatives as dual inhibitors for acetylcholinesterase and amyloid beta aggregation, *Bioorgan. Med. Chem. 20*, 2527-2534.

25. Ma, F., and Du, H. (2017) Novel deoxyvasicinone derivatives as potent multitarget-directed ligands for the treatment of Alzheimer's disease: Design, synthesis, and biological evaluation, *Eur. J. Med. Chem. 140*, 118.

26. Shidore, M., Machhi, J., Shingala, K., Rumkar, P. M., Sharma, M. K., Agrawal, N., Tripathi, A., Parikh, Z., Pillai, P., and Yadav, M. R. (2016) Benzylpiperidine-Linked Diarylthiazoles as Potential Anti-Alzheimer's Agents: Synthesis and Biological Evaluation, *J. Med. Chem. 59*, 5823-5846.

27. Ismaili, L., Refouvelet, B., Benchekroun, M., Brogi, S., Brindisi, M., Gemma, S., Campiani, G., Filipic, S., Agbaba, D., Esteban, G., Unzeta, M., Nikolic, K., Butini, S., and Marco-Contelles, J. (2017) Multitarget compounds bearing tacrine- and donepezil-like structural and functional motifs for the potential treatment of Alzheimer's disease, Prog. Neurobiol. *151*, 4-34.

28. Panek, D., Wieckowska, A., Jonczyk, J., Godyn, J., Bajda, M., Wichur, T., Pasieka, A., Knez, D., Pislar, A., Korabecny, J., Soukup, O., Sepsova, V., Sabate, R., Kos, J., Gobec, S., and Malawska, B. (2018) Design, Synthesis, and Biological Evaluation of 1-Benzylamino-2-hydroxyalkyl Derivatives as New Potential Disease-Modifying

Multifunctional Anti-Alzheimer's Agents, *Acs Chem. Neurosci. 9*, 1074-1094.

29. Iraji, A., Firuzi, O., Khoshneviszadeh, M., Tavakkoli, M., Mandavi, M., Nadri, H., Edraki, N., and Miri, R. (2017) Multifunctional iminochromene-2H-carboxamide derivatives containing different aminomethylene triazole with BACE1 inhibitory, neuroprotective and metal chelating properties targeting Alzheimer's disease, *Eur. J. Med. Chem. 141*, 690-702.
30. Bandyopadhyay, S., Huang, X., Cho, H., Greig, N.H., Youdim, M.B., Rogers, J.T. (2006) Metal specificity of an iron-responsive element in Alzheimer's APP mRNA 5'untranslated region, tolerance of SH-SY5Y and H4 neural cells to desferrioxamine, clioquinol, VK-28, and a piperazine chelator, *J. Neural. Transm. Suppl.* (71), 237-47.
31. Edraki, N., Firuzi, O., Foroumadi, A., Miri, R., Madadkar-Sobhani, A., Khoshneviszadeh, M., and Shafiee, A. (2013) Phenylimino-2H-chromen-3-carboxamide derivatives as novel small molecule inhibitors of beta-secretase (BACE1), *Bioorgan. Med. Chem. 21*, 2396-2412.
32. Lee, S., Zheng, X., Krishnamoorthy, J., Savelieff, M. G., Park, H. M., Brender, J. R., Kim, J. H., Derrick, J. S., Kochi, A., Lee, H. J., Kim, C., Ramamoorthy, A., Bowers, M. T., and Lim, M. H. (2014) Rational Design of a Structural Framework with Potential Use to Develop Chemical Reagents That Target and Modulate Multiple Facets of Alzheimer's Disease, *J Am. Chem. Soc. 136*, 299-310.
33. Ellman, G. L., Courtney, K. D., Andres, V., Jr., and Feather-Stone, R. M. (1961) A new and rapid colorimetric determination of acetylcholinesterase activity, *Biochem. pPharmacol. 7*, 88-95.
34. Bartolini, M., Bertucci, C., Bolognesi, M. L., Cavalli, A., Melchiorre, C., and Andrisano, V. (2007) Insight into the kinetic of amyloid beta(1-42) peptide self-aggregation: Elucidation of inhibitors' mechanism of action, *Chembiochem 8*, 2152-2161.
35. Mosmann, T. (1983) Rapid colorimetric assay for cellular growth and survival: application to proliferation and cytotoxicity assays, *J. Immunol. Methods 65*, 55-63.

36. Lipinski, C. A. (2004) Lead- and drug-like compounds: the rule-of-five revolution, *Drug Discov. Today. 1*, 337-341.

37. Clark, D. E. (1999) Rapid calculation of polar molecular surface area and its application to the prediction of transport phenomena. 2. Prediction of blood-brain barrier penetration, *J. Pharm. Sci. 88*, 815-821.

38. Cheung, J., Rudolph, M. J., Burshteyn, F., Cassidy, M. S., Gary, E. N., Love, J., Franklin, M. C., and Height, J. J. (2012) Structures of Human Acetylcholinesterase in Complex with Pharmacologically Important Ligands, *J J. Med. Chem. 55*, 10282-10286.

39. Rueeger, H., Lueoend, R., Rogel, O., Rondeau, J.-M., Moebitz, H., Machauer, R., Jacobson, L., Staufenbiel, M., Desrayaud, S., and Neumann, U. (2012) Discovery of Cyclic Sulfone Hydroxyethylamines as Potent and Selective beta-Site APP-Cleaving Enzyme 1 (BACE1) Inhibitors: Structure-Based Design and in Vivo Reduction of Amyloid beta-Peptides, *J. Med. Chem. 55*, 3364-3386.

40. Crescenzi, O., Tomaselli, S., Guerrini, R., Salvadori, S., D'Ursi, A. M., Temussi, P. A., and Picone, D. (2002) Solution structure of the Alzheimer amyloid beta-peptide (1-42) in an apolar microenvironment - Similarity with a virus fusion domain, *Eur. J. Med. Chem. 269*, 5642-5648.

41. PyMOL 0.99rc6, DeLano Scientific LLC: Palo Alto, CA, USA, 2006.

Table 1.

Inhibition of *h*AChE, *h*BuChE, BACE-1 and Aβ_{1-42} aggregation by the synthesized compounds.

Compound	IC_{50} (nM)[a] or inhibition % at 1 μM		S.I. [b]	IC_{50} (μM)[a] for BACE-1 or inhibition % at 10 μM	IC_{50} (μM)[a] for Aβ_{1-42} or inhibition % at 20 μM
	*h*AChE	*h*BuChE			
8a	423.82 ± 11.46	35.22 %	> 2.3	22.53 %	46.35 %
8b	77.29 ± 1.82	832.63 ± 28.33	10.7	0.257 ± 0.01	20.15 %
8c	706.78 ± 25.43	38.45 %	> 1.4	35.55 %	40.33 %
8d	37.55 %	30.28 %	n.d. [c]	28.74 %	25.33 %
9a	23.85 ± 0.82	48.24 %	> 41.9	0.028 ± 0.002	25.26 %
9b	20.44 ± 0.23	687.55 ± 18.58	33.6	0.71 ± 0.03	36.16 %
9c	92.75 ± 2.87	43.79 %	> 10.7	1.35 ± 0.05	22.98 %
9d	648.92 ± 22.45	942.68 ± 26.71	1.4	45.62 %	36.26 %
10a	56.14 ± 2.08	47.28 %	> 17.8	0.834 ± 0.02	13.26 ± 0.57
10b	45.65 ± 1.75	532.75 ± 10.88	11.6	0.681 ± 0.03	22.34 %
10c	538.48 ± 27.85	46.56 %	> 1.8	0.085 ± 0.003	42.15 %
10d	5.91 ± 0.15	493.25 ± 11.35	83.4	0.167 ± 0.005	19.43 ± 0.62
11a	3.29 ± 0.11	45.3 %	> 303	0.129 ± 0.003	9.26 ± 0.37
11b	10.28 ± 0.24	198.42 ± 6.84	19.2	0.543 ± 0.02	28.68 %
11c	16.42 ± 0.46	42.45 %	> 60.9	2.59 ± 0.08	30.88 %
11d	43.62 %	792.62 ± 22.68	0.7	0.595 ±0.03	32.59 %
11e	73.58 ± 2.09	39.67 %	>13.5	43.20 %	30.12 %
11f	11.76 ± 0.31	48.36 %	> 85.0	32.62 %	31.25 %
11g	758.74 ± 18.64	43.66 %	> 1.3	8.92 ± 0.34	27.44 %
11h	23.91 %	40.41 %	n.d. [c]	4.92 ± 0.15	22.67 %
11i	67.45 ± 2.25	45.42 %	> 14.8	6.25 ± 0.30	31.84 %
11j	8.65 ± 0.27	48.95 %	> 115.6	9.03 ± 0.29	5.41 ± 0.15
11k	214.89 ± 4.16	42.59 %	> 4.6	38.15 %	23.69 %
11l	39.66 %	46.91 %	n.d. [c]	0.915 ± 0.03	43.26 %
11m	105.42 ±3.68	758.12 ± 25.36	7.1	22.04 %	27.32 %
Tacrine	76.53 ± 3.12	10.84 ± 1.36	0.1	n.d. [c]	n.d. [c]
Donepezil	18.54 ± 1.02	19.73 %	> 53.9	n.d. [c]	n.d. [c]
OM99-2	n.d. [c]	n.d. [c]	n.d.	0.016 ± 0.002	n.d. [c]
Resveratrol	n.d. [c]	n.d. [c]	n.d.	n.d. [c]	10.92 ± 0.42
Curcumin	n.d. [c]	n.d. [c]	n.d.	n.d. [c]	14.25 ± 0.58

[a] Values are expressed as mean ± SD of five independent experiments.

[b] Selectivity index for AChE is defined as IC_{50} (*h*BuChE) / IC_{50} (*h*AChE).

[c] n.d. Not determined.

Table 2.

Physiochemical properties of compounds **10a, 10d, 11a, 11j**, tacrine, donepezil, resveratrol and curcumin.

Compound	M.W. [a]	HBA [b]	HBD [b]	Rot. bonds [b]	tPSA [a]	cLog *P* [a]	LogBB [c]
10a	459.59	7	1	8	68.25	3.63	-0.32
11a	417.51	7	1	5	68.25	3.14	-0.39
11j	431.54	7	1	5	68.25	3.55	-0.33
Tacrine	198.27	2	2	0	36.16	2.27	-0.05
Donepezil	379.50	4	0	6	38.77	4.60	-0.26
Resveratrol	228.25	3	3	2	60.69	2.83	-0.33
Curcumin	368.38	6	2	8	93.06	2.25	-0.9
Required parameters [d]	< 500	< 10	< 5	< 10	< 90	2-5	> -1

[a] Calculated using ChemBioDraw Ultra14.0. M.W.: molecular weight; tPSA: total polar surface area; cLog P: log octanol/water partition coefficient.

[b] Calculated using Cheminformatics (http://www.molinspiration.com). HBA: number of hydrogen acceptors; HBD: number of hydrogen donors; Rot. bonds: number of rotatable bonds.

[c] $\text{LogBB} = -0.0148 \times \text{tPSA} + 0.152 \times \text{cLogP} + 0.139$. [92]

[d] Required parameters necessary to fulfill appropriate physiochemical properties as judged appropriate according to Lipinski's rules and those important for BBB permeation [91-93].

Scheme 1.

Synthesis of compounds **8*a*–11*m***.

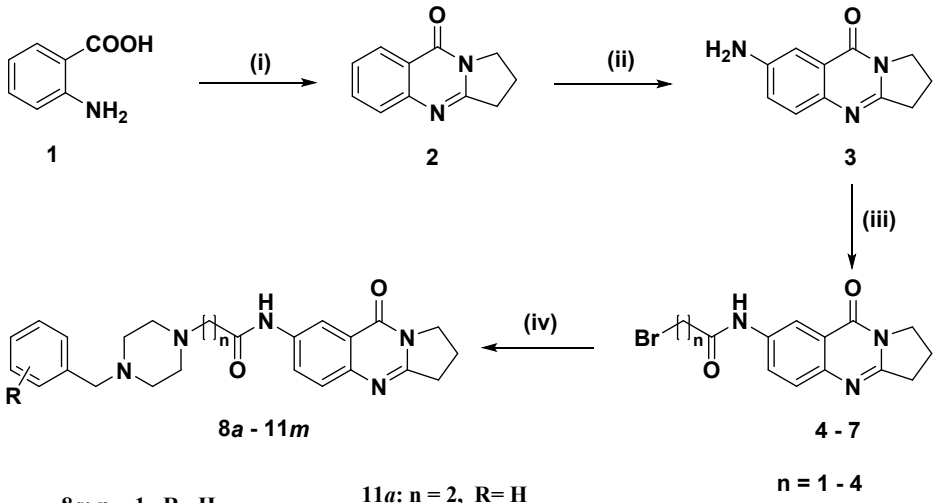

8*a*: n = 1, R= H
8*b*: n = 1, R= *p* - CH_3
8*c*: n = 1, R= *p* - F
8*d*: n = 1, R= *p* - CF_3
9*a*: n = 3, R= H
9*b*: n = 3, R= *p* - CH_3
9*c*: n = 3, R= *p* - F
9*d*: n = 3, R= *p* - CF_3
10*a*: n = 4, R= H
10*b*: n = 4, R= *p* - CH_3
10*c*: n = 4, R= *p* - F
10*d*: n = 4, R= *p* - CF_3

11*a*: n = 2, R= H
11*b*: n = 2, R= *p* - CH_3
11*c*: n = 2, R= *p* - F
11*d*: n = 2, R= *p* - CF_3
11*e*: n = 2, R= *p* - Cl
11*f*: n = 2, R= *m* - CH_3
11*g*: n = 2, R= *m* - F
11*h*: n = 2, R= *m* - CF_3
11*i*: n = 2, R= *m*- Cl
11*j*: n = 2, R= *o* - CH_3
11*k*: n = 2, R= *o* - F
11*l*: n = 2, R= *o* - CF_3
11*m*:n = 2, R= *o*- Cl

Reagents and conditions: (i) $POCl_3$, dry toluene. (ii) a) HNO_3, H_2SO_4, rt.; (b) $Na_2S{\cdot}9H_2O$, NaOH, EtOH, reflux;. (iii) Different bromoacid derivatives, EDCI, dry CH_2Cl_2, reflux;. (iv) Piperazine derivative, $NaHCO_3$, EtOH, reflux.

Legend of Figures

Figure 1. Deoxyvasicinone and its derivatives [21,24,25].

Figure 2. Design strategy for the new series of donepezi-deoxyvasicinone derivatives targeting AChE, BACE-1 and A$\beta_{1\text{-}42}$ aggregation[30].

Figure 3. AChE induced A$\beta_{1\text{-}42}$ aggregation inhibition by compounds **10*a***, **11*a*** and **11*j***. Data are represented as mean ± SD of five independent experiments. *** $p < 0.001$ *vs* control group.

Figure 4. Kinetic study on the mechanism of *h*AChE inhibition by compound **11*a***. Lineweaver-Burk plot of AChE showing competitive inhibition with various concentrations of **11*a*** (1 nM, 5 nM, 10 nM) in different substrate concentrations (0.1 - 0.5 mM).

Figure 5. Neurotoxicity of compounds in (A) SH-SY5Y and (B) HepG2 cells. Data are represented as mean ± SD of five independent experiments. *$p < 0.05$, **$p < 0.01$ and *** $p < 0.001$ *vs* control group (untreated cells).

Figure 6. Neuroprotective effects of compounds **10*a***, **11*a*** and **11*j*** against A$\beta_{1\text{-}42}$-induced cell death in SH-SY5Y cells. Data are represented as mean ± SD of five independent experiments.$^{\#\#\#}$ $p < 0.001$ *vs* control group (untreated cells); **$p < 0.01$, ***$p < 0.001$ *vs* A$\beta_{1\text{-}42}$-treated cells.

Figure 7. Proposed binding mode of compound **11*a*** in the active site of (A) AChE (PDB: 4ey7), (B) BACE-1 (PDB: 4d8c) and (C) A$\beta_{1\text{-}42}$ ((PDB: 1iyt). The blue dashed lines represent hydrogen bonds, the red dashed lines stand for π-π *or* π-cation interactions. The figures were made with PyMol (http://www.pymol.org).

Figure 1.

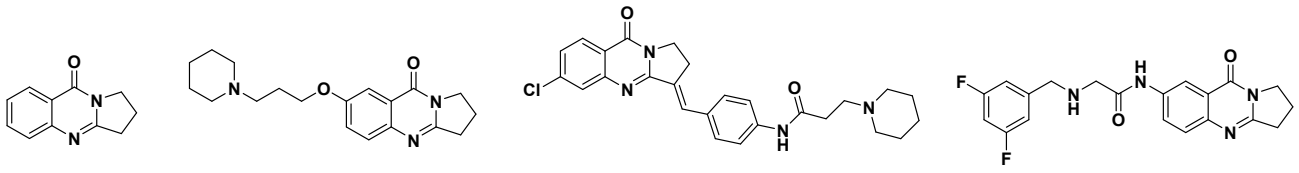

I
Deoxyvasicinone

II
IC_{50} (*ee*AChE) = 50 nM

III
IC_{50} (*ee*AChE) = 23 nM

IV
IC_{50} (*h*AChE) = 7.6 nM

Figure 2.

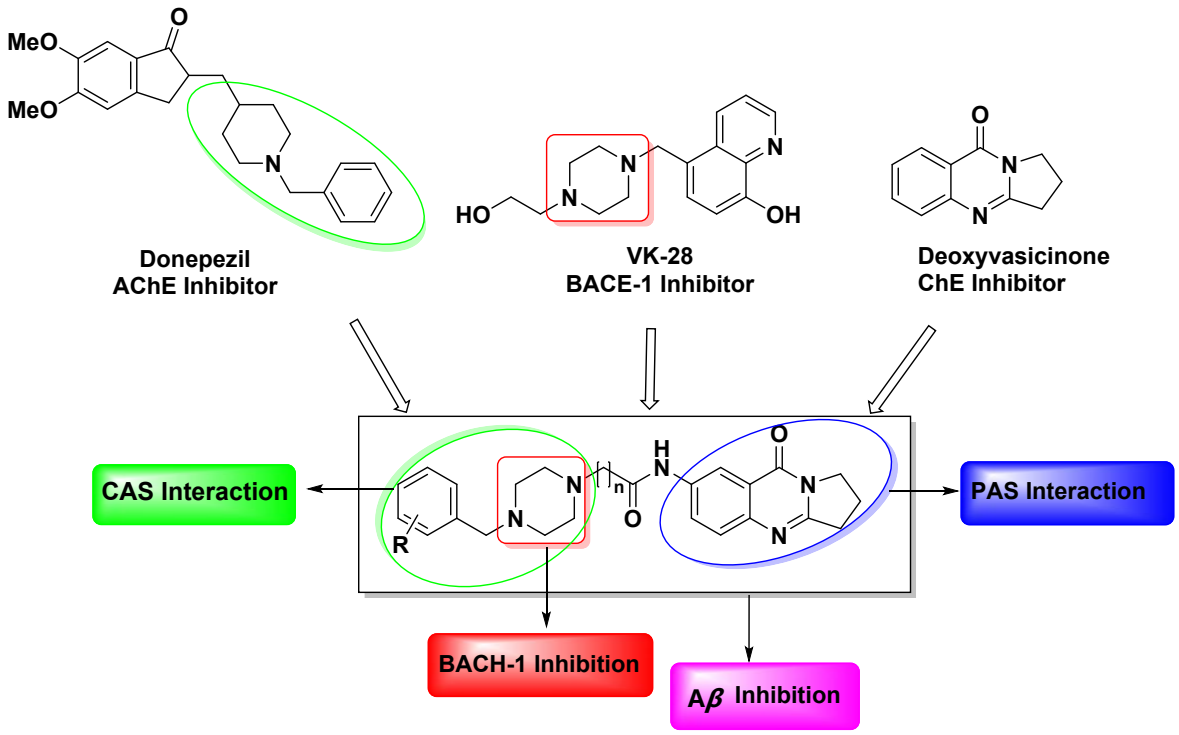
MeO
MeO
O
N
Donepezil
AChE Inhibitor
HO
N
N
N
OH
VK-28
BACE-1 Inhibitor
O
N
N
Deoxyvasicinone
ChE Inhibitor
CAS Interaction
R
N
N
n
H
N
O
O
N
N
PAS Interaction
BACH-1 Inhibition
Aβ Inhibition

Figure 3.

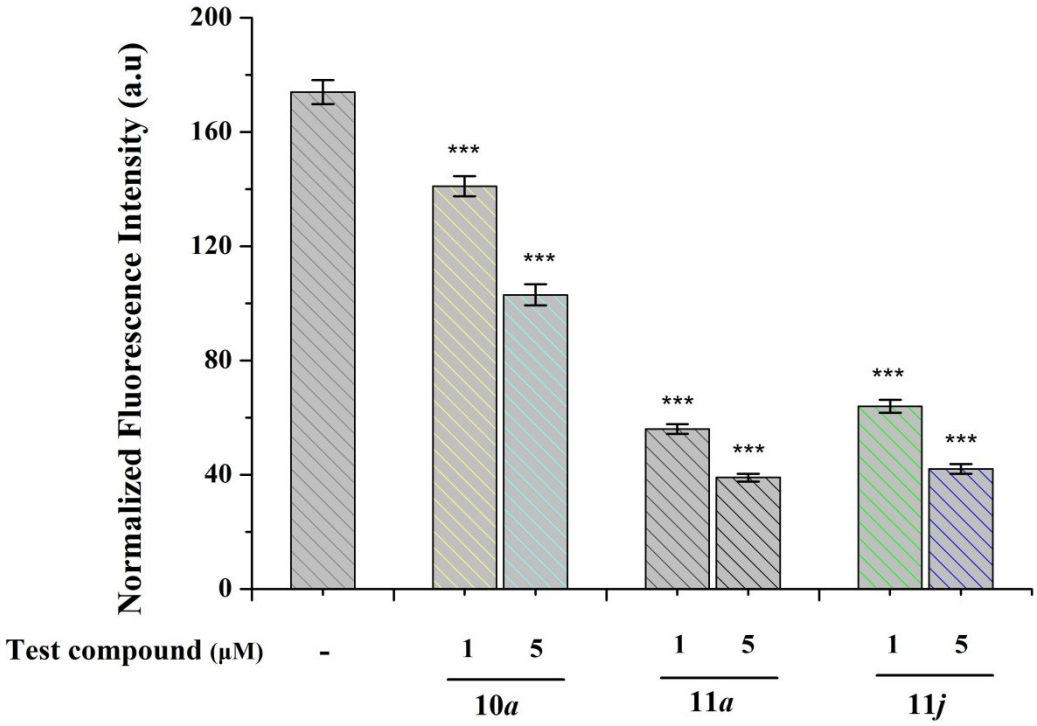
Normalized Fluorescence Intensity (a.u)
200
160
120
80
40
0
***
***
***
***
***
***
Test compound (μM)
-
1
5
1
5
1
5
10a
11a
11j

Figure 4.

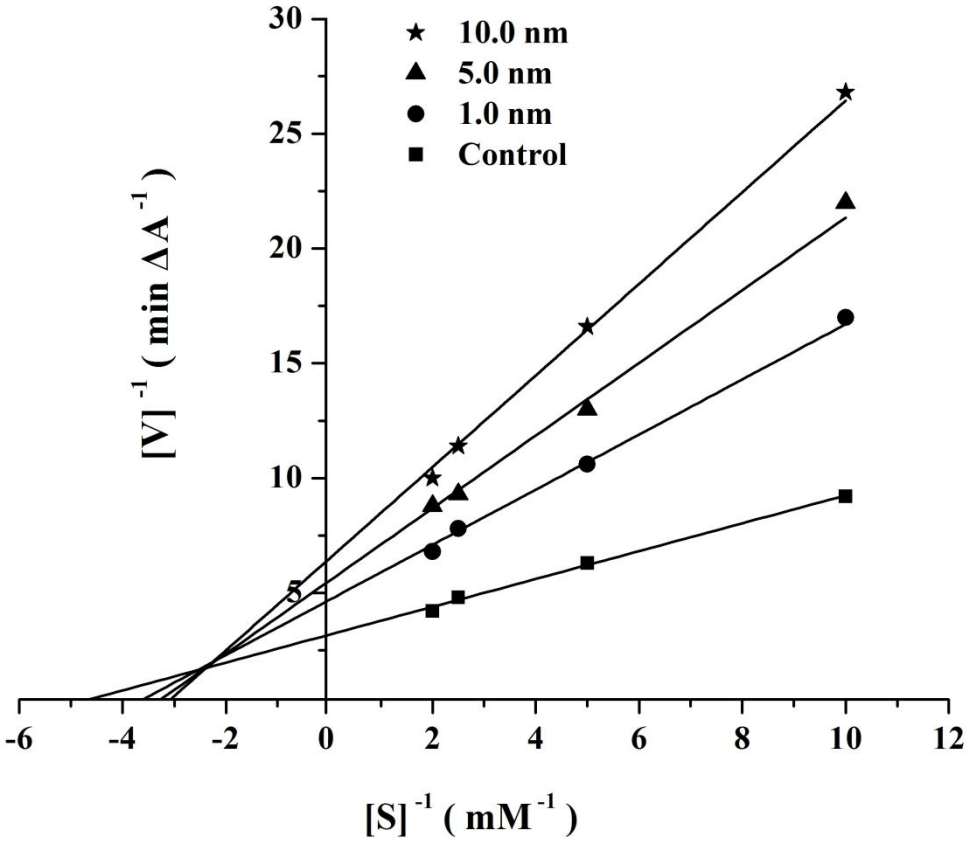
10.0 nm
5.0 nm
1.0 nm
Control
[V] -1 (min ΔA -1)
[S] -1 (mM -1)
30
25
20
15
10
5
-6
-4
-2
0
2
4
6
8
10
12

Figure 5.

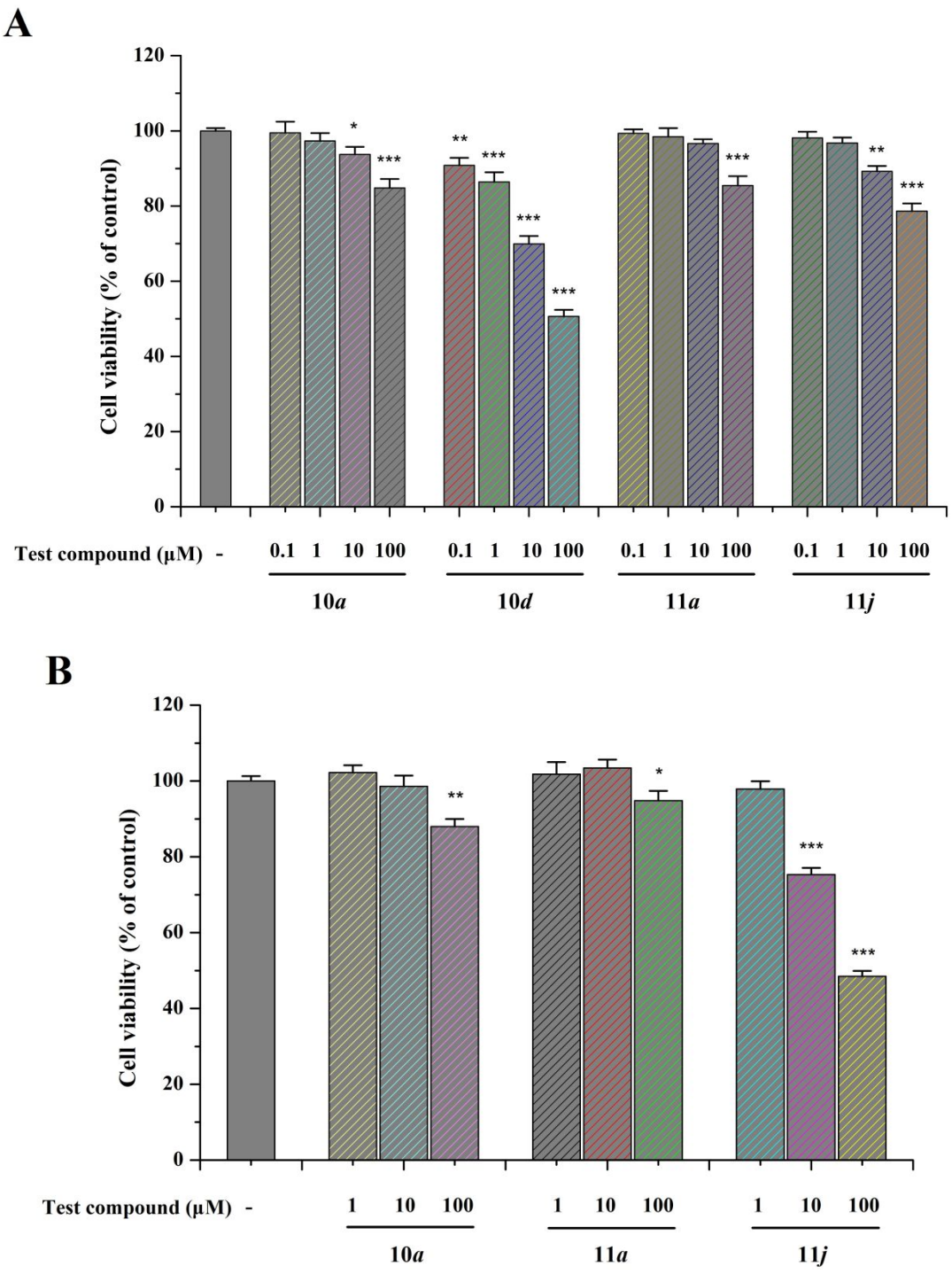
A
Cell viability (% of control)
120
100
80
60
40
20
0
*
**
***
Test compound (μM) -
0.1 1 10 100
10a
10d
11a
11j
B
Cell viability (% of control)
1 10 100
10a
11a
11j

Figure 6.

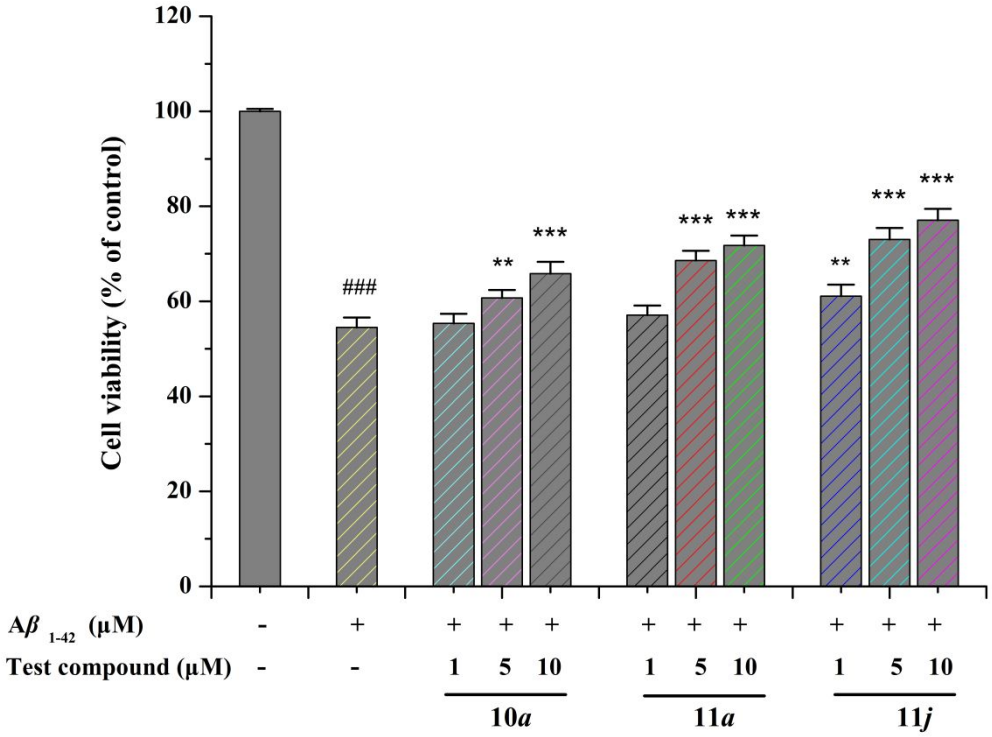
Cell viability (% of control)
120
100
80
60
40
20
0
###
**
***
***
***
**
***
***
Aβ 1-42 (μM) - + + + + + + + + + + +
Test compound (μM) - - 1 5 10 1 5 10 1 5 10
10a
11a
11j

Figure 7.

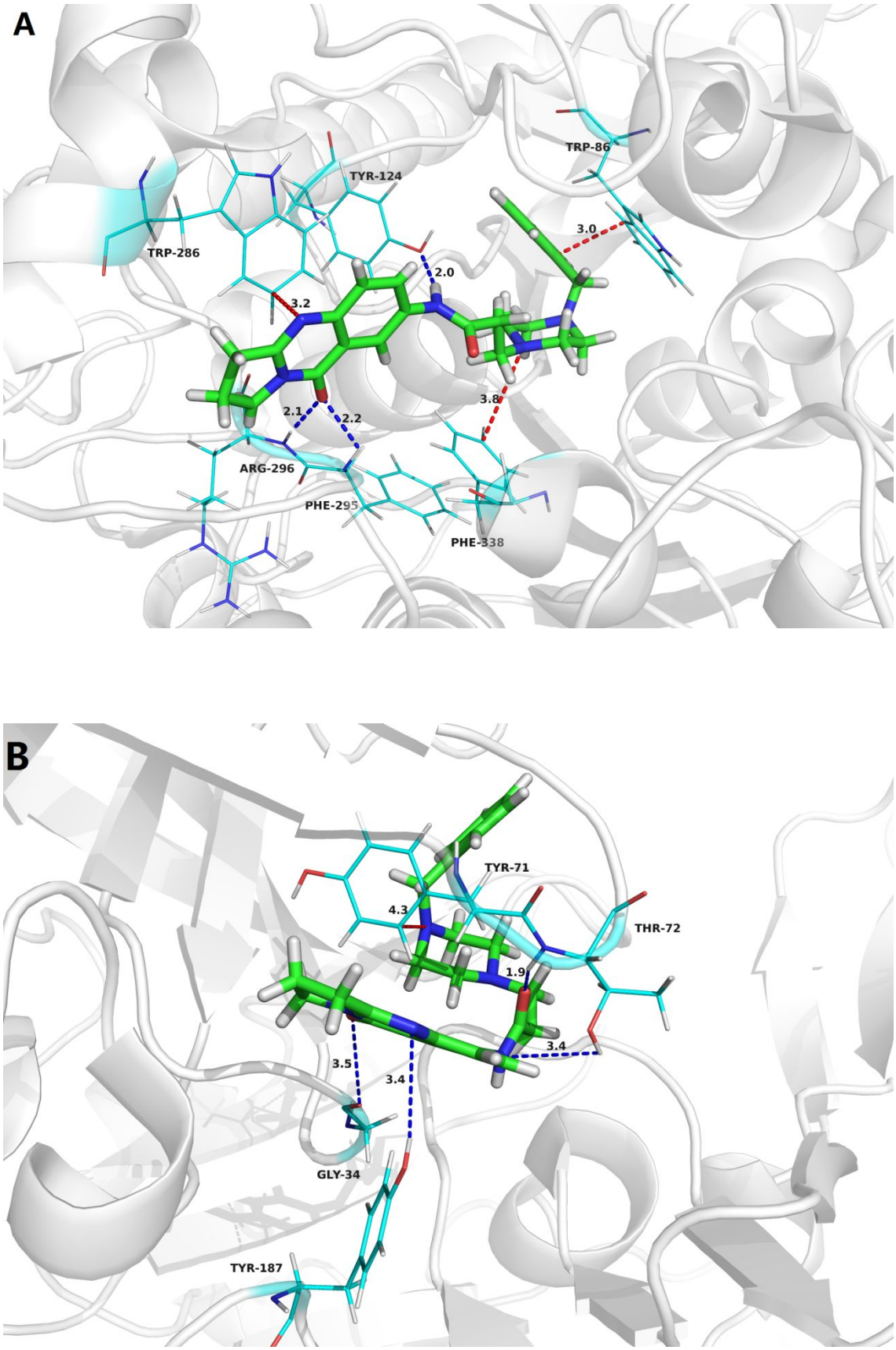
A
TRP-86
TYR-124
TRP-286
3.0
2.0
3.2
3.8
2.1
2.2
ARG-296
PHE-295
PHE-338
B
TYR-71
4.3
THR-72
1.9
3.4
3.5
3.4
GLY-34
TYR-187

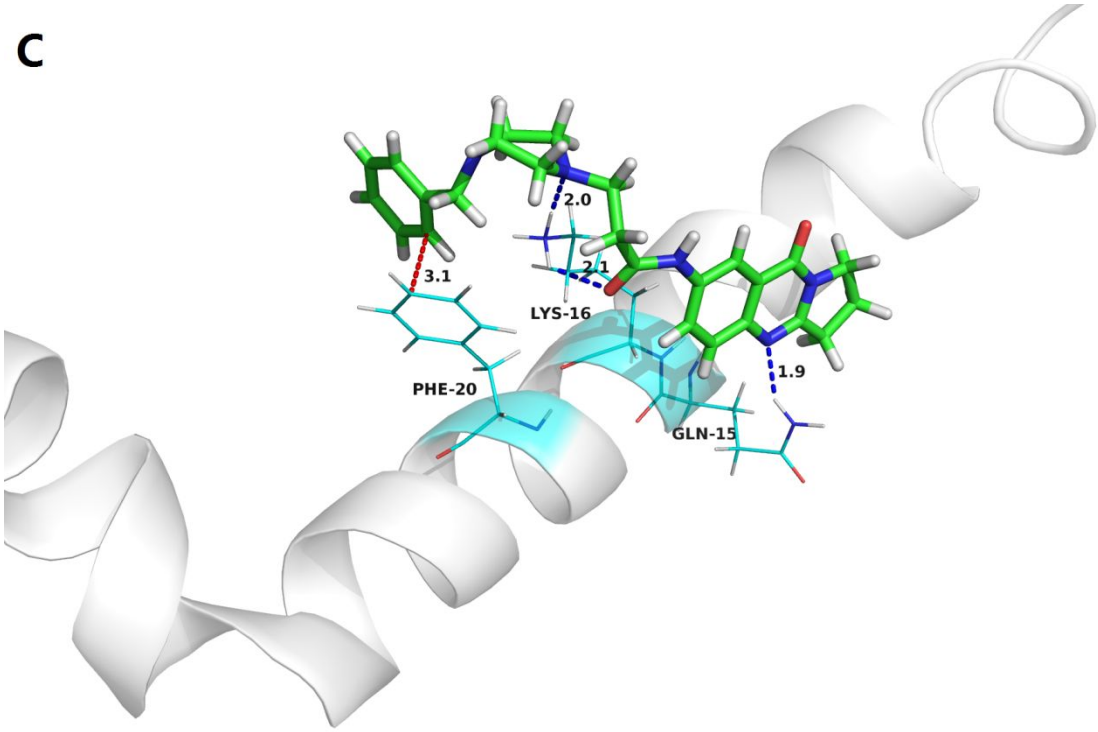
C
2.0
2.1
3.1
LYS-16
PHE-20
1.9
GLN-15

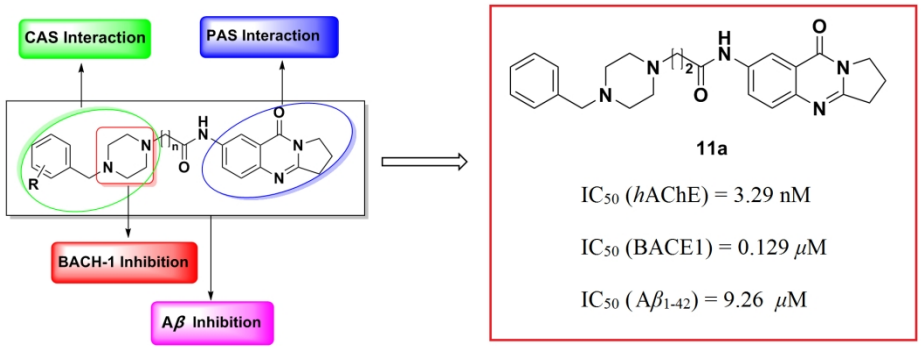

461x171mm (120 x 120 DPI)